SECTION

THE JOHNS HOPKINS UNIVERSITY
APPLIED PHYSICS LABORATORY
8621 GEORGIA AVE., SILVER SPRING, MD.

Operating under Contract NOrd 7386
With the Bureau of Ordnance, U. S. Navy

AD 634865

AERODYNAMIC CHARACTERISTICS OF WINGS AT SUPERSONIC SPEEDS

by

R. M. Snow and E. A. Bonney

CLEARINGHOUSE
FOR FEDERAL SCIENTIFIC AND
TECHNICAL INFORMATION
Hardcopy Microfiche
$6.00 $.75 67 pp
ARCHIVE COPY

DDC
JUL 11 1966

Bumblebee Series
Report No. 55
Copy No. 218

March 1947

DISTRIBUTION OF THIS
DOCUMENT IS UNLIMITED

ACCESSION for
CFSTI
BDC
UNANNOUNCED
JUSTIFICATION
BY
DISTRIBUTION/AVAILABILITY CODES
DIST. | AVAIL. and/or SPECIAL
1

THE JOHNS HOPKINS UNIVERSITY
APPLIED PHYSICS LABORATORY

8621 Georgia Avenue
Silver Spring, Maryland

Operating Under Contract NOrd 7386
With the Bureau of Ordnance, U.S. Navy

AERODYNAMIC CHARACTERISTICS OF WINGS AT SUPERSONIC SPEEDS

by

R. M. Snow and E. A. Bonney

BUMBLEBEE Report No. 55

DISTRIBUTION OF THIS
DOCUMENT IS UNLIMITED

MARCH
1947

TABLE OF CONTENTS

Introduction. v
Reference Table for Aerodynamic Coefficients. vi

I. Application of Busemann's Conical Field Method to Thin Wings by Robert M. Snow

Introduction. 1
Characteristic Cones, Boundary Conditions 3
Rectangular Wing. 4
Raked Wing. 8
Bent Leading Edge 11
Case of Intersecting Envelopes. 13
Trapezoidal Wing. 15
General Symmetrical Quadrilateral 16
Wing With Dihedral. 20

II. Aerodynamic Characteristics of Solid Rectangular Airfoils at Supersonic Speeds by E. A. Bonney

Summary. 23
Assumptions 23
Nomenclature. 24
Discussion. 26
Derivations 27
Results 34
Conclusions 34

III. The Reverse Delta Planform. 43

IV. Lift and Drag Characteristics of Delta Wings at Supersonic Speeds by E. A. Bonney

Abstract. 44
Assumptions 45
Nomenclature. 45
Discussion. 46

V. Sectional Characteristics of Standard Airfoils by E. A. Bonney. 58

LIST OF FIGURES

I. Application of Busemann's Conical Field Method to Thin Wings

Figure 1. Flow for Rectangular Wing, Section by Plane Perpendicular to Stream 3
2. Flow for Swept-back Leading Edge. 4
3. Pressure Distribution Along Span for Rectangular Wing or for Raked-back Rectangular Wing 7
4. Wing With Dihedral, Section by Plane Perpendicular to Stream 14
5. Symmetrical Trapezoidal Wing. 15
6. Pressure Distribution Along a Span Line for Trapezoid 16
7. Pressure Distribution Along Span Line for Forward-pointing Triangle 17
8. General Quadrilateral 17
9. Wing With Dihedral. 20

II. Aerodynamic Characteristics of Solid Rectangular Airfoils at Supersonic Speeds

Figure 1. Pressure Loss Due to Flow Around the Tip. 38
2. C_3 vs M 38
3. Aspect Ratio Correction to Lift and Wave Drag 38
4. Center of Pressure for Finite Aspect Ratio. 38
5. K_λ's for Various Wing Sections (single taper) 39
6. K_λ's for Various Wing Sections (double taper) 39
7. Aspect Ratio for Thin Rectangular Wings Supported Over Entire Base. 39
8. Optimum Lift Coefficient - Entire Base. 39
9. Maximum Lift-Drag Ratio - Entire Base 40
10. Optimum Angle of Attack - Entire Base 40
11. Lift Curve Slope - Entire Base. 40
12. Thickness Ratio - Entire Base 40
13. Optimum Aspect Ratios for Thin Rectangular Wings Supported by a Hub. 41
14. Optimum Lift Coefficient - Hub. 41
15. Maximum Lift-Drag Ratio - Hub 41
16. Optimum Angle of Attack - Hub 41
17. Lift Curve Slope - Hub. 42
18. Thickness Ratio - Hub 42

IV. Lift and Drag Characteristics of Delta Wings at Supersonic Speeds

Figure 1. Lift Characteristics of Delta Wings. 50
2. Form Drag of Delta Airfoils Whose Leading Edges are Inside the Mach Cone 50
3. Lift-Drag Ratio of Delta and Rectangular Wings 51
4. Maximum Lift-Drag Ratio - Delta Wings. 51
5. Maximum Lift-Drag Ratio 51
6. Optimum Angle of Attack - Delta Wings. 51
7. Ratio of Maximum Lift-Drag Ratios of Delta and Reverse Arrow Wings. 52
8. Aspect Ratio of Delta Wings. 52
9. Planform Semi-vertex Angle of Delta Wings. 52
10. Optimum Lift Coefficient - Delta Wings 52
11. Optimum Lift Coefficient 53
12. Spanwise Center of Pressure Location - Delta Wings 53
13. (Nomenclature) 53
14. Delta Wing Drag vs Maximum Thickness Position, Swept Trailing Edge; a = 0.5 53
15. Delta Wing Drag vs Sweepback Angle, Swept Trailing Edge; a = 0 54
16. Delta Wing Drag vs Sweepback Angle, Swept Trailing Edge; a = 0.5 54
17. Delta Wing Drag vs Sweepback Angle, Swept Trailing Edge; b = 0.2 55
18. Delta Wing Drag vs Mach Number, Swept Trailing Edge; b = 0.2 55
19. Lift Curve Slope - Delta and Arrowhead Planforms 56
20. Lift Curve Slope - Delta and Arrowhead Planforms 56
21. Spanwise Center of Pressure Location - Delta and Arrowhead Planforms. 57
22. Chordwise Center of Pressure Location - Delta and Arrowhead Planforms. 57

V. Sectional Characteristics of Standard Airfoils

Figure 1. Drag Coefficient vs Stress 59
2. Drag Coefficient vs Thickness Ratio. 60
3. Stress vs Thickness 60

INTRODUCTION

Five papers dealing with practical aspects of theoretical work done at the Applied Physics Laboratory on the subject of the aerodynamic characteristics of wings in supersonic flow are presented in this BUMBLEBEE report. These papers, which have appeared as internal memoranda of the Applied Physics Laboratory, represent the combined efforts of APL/JHU personnel and outside contributors as noted in the references.

The first paper derives lift coefficients and center of pressure location for flat plates of polygonal planform from fundamental considerations, using Busemann's conical field method. The other papers utilize Busemann's second order approximation formula to determine the aerodynamic characteristics of certain types of wings having finite thickness. Consequently there will be some overlapping of results, but no material is deleted inasmuch as the two methods are quite different. Attention is called, however, to differences in nomenclature between the first and the remaining papers. A short discussion of the sectional properties of various airfoil shapes and the optimum type is given at the end of this report.

It is believed that these papers cover most of the unclassified engineering work on the effect of wing planforms available at this time. The work is by no means complete, there being many practical planforms for which no theory has been developed, particularly in the case of wings with finite thickness. Accordingly the table on the following page has been constructed to indicate the types for which information can be found in this report, to show where it can be found, and to indicate the missing data. In this table the Roman numeral refers to the paper in this report as indexed in the Table of Contents, whereas the Arabic numeral refers to the page on which the expression for the particular coefficient may be found. An X indicates that the exact information is not yet known.

REFERENCE TABLE FOR AERODYNAMIC COEFFICIENTS

		1	2	3a	3b	4	5a	5b	6a	6b	7a	7b	8	9
Description		Infinite Span	Rectangular	Raked Tip or Trapezoidal 1	Raked Tip or Trapezoidal 2	Reversed Delta *	Delta 1	Delta 2	Diamond 1	Diamond 2	Arrow 1	Arrow 2	Reverse Arrow	Modified Diamond (Low AR)
Sketch + Airflow →		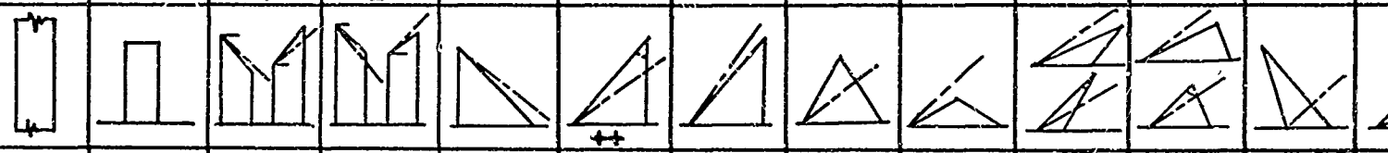												
Flat Plate	C_L	II-37	I-7 II-37	I-10,15	I-10,15	X***	I-16 IV-50	IV-52	I-19++ IV-56	IV-56	I-18++ IV-56	+++ IV-56	I-18	X
	C_{D_o}													
	C_M	II-37	I-7 II-37	I-10,15	I-10,15	X***	I-16	X	I-19 IV-57	IV-57	I-18 IV-57	X	I-18	X
	c.p.	II-37	I-7 II-37	I-10,15	I-10,15	X***	I-16		I-19 IV-57	IV-57	I-18 IV-57	X	I-18	X
Airfoil	C_L	II-37	II-37	X **	X	X **	IV-50	IV-50 **	IV-56 **	IV-56	IV-56 **	IV-56	X **	X
	C_{D_o}	II-37	II-37	X	X	IV-54	IV-50	IV-50	X	X	IV-53, 54, 55	X	X	X
	C_M	II-37	II-37	X	X	X	IV-57	IV-57	IV-57	IV-57	IV-57	IV-57	X	X
	c.p.	II-37	II-37	X	X	X	IV-57	IV-57	IV-57	IV-57	IV-57	IV-57	X	X

(Roman and arabic numerals refer to section and page.)

* Sometimes called "reverse arrow".

\+ Constant thickness ratio spanwise was assumed for all triangular wings and for raked tip wings beyond the limit of the shortest edge (leading or trailing).

** Will be very close to value for flat plate.

++ Case of the raked tip (indicated by dotted line) out of the Mach cone from the tip can also be determined for these types.

*** Lift is two-dimensional and/or center of pressure is at centroid of area.

I. APPLICATION OF BUSEMANN'S CONICAL FIELD METHOD TO THIN WINGS*

by Robert M. Snow

Introduction

In this paper the pressure distribution, lift coefficient and center of pressure are determined for several plane wings of polygonal planform at small angles of attack, by the method of "conical fields". The effect of a dihedral bend is also obtained. Squares and products of perturbation velocities have been neglected, since the method is based on the Prandtl-Glauert linearized potential equation. Modifications due to wing thickness, viscous effects, and interference effect (with a fuselage or with other wings) are likewise neglected.

The method of conical fields in supersonic aerodynamics was developed by Busemann (Ref. 1), who applied it to several important problems. Stewart (2) has solved the problem of a delta wing by essentially the same method. A conical field corresponds to a linear homogeneous solution of the linearized (or Prandtl-Glauert) potential equation for supersonic flow:

$$\frac{\partial^2 \Phi}{\partial x^2} + \frac{\partial^2 \Phi}{\partial y^2} - (M^2-1)\frac{\partial^2 \Phi}{\partial z^2} = 0 \qquad (1)$$

Here M is the Mach number of the main stream, which is moving along the z - axis. The perturbation velocity components (u, v, w) are also solutions of Eq. (1) and are homogeneous of degree zero, i.e., u, v, and w are constant along any ray emanating from the origin. The particular simplicity of conical fields lies in the fact that after a transformation the perturbation velocity components (u, v, w) are obtained as solutions of Laplace's equation in two variables. Busemann credits this transformation to Chaplygin, (3) who made use of it in a formally similar problem. Since the general theory has been discussed recently by Stewart (2) it is only needed to state the principal result in the form in which it will be

---

* This paper is a revision of CM-265 originally published as an internal memorandum of the Applied Physics Laboratory.

** Lift is two-dimensional and/or center of pressure is at centroid of area.

utilized. Let μ be the Mach angle ($\sin^{-1} 1/M$), and x, y, z a rectangular coordinate system with the z - axis pointing downstream, and

$$\varphi = \tan^{-1} y/x \qquad R = \frac{\sqrt{x^2+y^2}}{z} \qquad A = \tan \mu$$

The transformation

$$\left.\begin{aligned} r &= \left\{\frac{1-\sqrt{1-R^2/A^2}}{1+\sqrt{1-R^2/A^2}}\right\}^{1/2} = \frac{A}{R} - \sqrt{\frac{A^2}{R^2}-1} \\ R &= \frac{2Ar}{1+r^2} \end{aligned}\right\} \tag{2}$$

is such that homogeneous functions of degree zero which satisfy Eq. (1) also satisfy Laplace's equation in the polar coordinates r, φ). The evaluation of the streamwise component (w) of perturbation velocity is of primary importance since the aerodynamic forces on the wing are determined by w alone. This follows from the linearized Bernoulli equation,

$$p = p - \rho W w \tag{3}$$

which, like Eq. (1), results from neglecting squares and products of perturbation velocities in the corresponding exact equation. In many problems of this type, including those considered here, w may be determined without further reference to the components u and v.

Characteristic Cones, Boundary Conditions

To illustrate the type of boundary condition needed to determine the conical field, consider the special case of a rectangular wing. This rectangular wing may be regarded as the result of cutting off the ends of a two-dimensional airfoil. This operation causes a modification in the flow (originally two-dimensional), which may be referred to as the "tip effect". In this connection, a fundamental distinction should be made between subsonic flow and supersonic flow. For subsonic flow (differential equation of elliptic type) the tip effect dies off asymptotically with increasing distance inboard. For supersonic flow (differential equation of hyperbolic type) the tip effect falls to zero at a certain finite distance, and the entire effect is contained within a region bounded by real characteristic surfaces. For linearized supersonic flow, the domain of influence of any point is bounded by a "Mach cone", which is one nappe of a cone opening downstream with semi-vertex angle equal to the Mach angle μ . Figure 1 represents a section by a plane perpendicular to the main stream. The Mach cones from the tips of the leading edge divide this plane into three types of regions. In the central region (I) the flow is in all respects the same as if the wing were of infinite span, because no point of this central region lies in the domain of influence of any point removed in the mental process of obtaining the rectangular wing from an airfoil of infinite span. On the other hand the perturbation velocity components are zero in the exterior region (III), because no point of this region lies in the domain of influence of any point on the rectangular wing. The requirement of continuity leads to boundary conditions which must be satisfied by the perturbation velocity components u, v and w on the boundary of each conical transition region (II). On the boundary between regions (II) and (III), u, v and w must vanish. On the boundary between regions (I) and (II), u, v and w take on the (constant, two-dimensional) values of region (I).

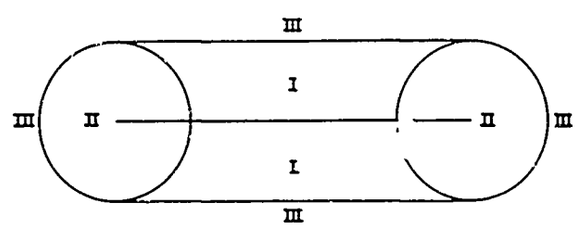

I Flow Same as for about Infinite Span Airfoil

II Conical Field

III Free Stream

FIG. I

FLOW FOR RECTANGULAR WING, SECTION BY PLANE PERPENDICULAR TO STREAM

Similar statements apply also to the example of a swept-back leading edge (Fig. 2). The two lines forming the leading edge are, of course,

finite in the actual case, but the effect of their finiteness will be confined by characteristic cones passing through the points at which the leading edge changes direction. The possibility of treating more general polygonal wings by this method follows from these remarks. For the polygons that may be treated by this method, there are isolated regions of uniform flow (identical with the flow for an infinite wing at a certain angle of yaw) separated by regions of transition in the Mach cones which start from each vertex of the polygon and open downstream. It is convenient in the following discussion to refer to these special Mach cones simply as "the Mach cones" or "the Mach cone".

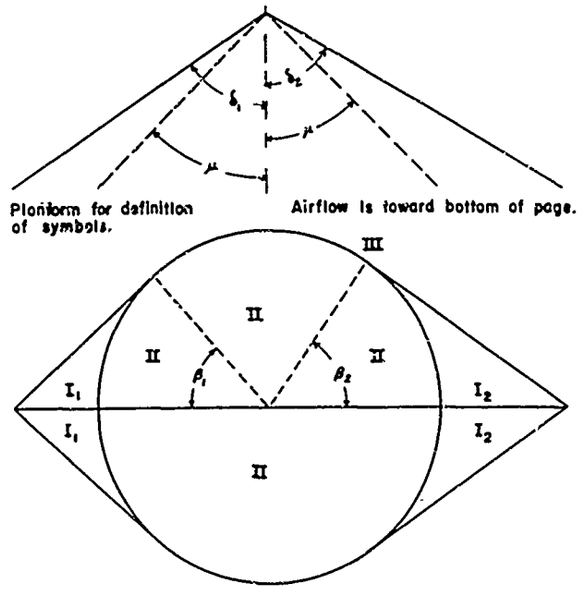

I_1 Flow same as for infinite span airfoil at angle of yaw $\pi/2 - \delta_1$
I_2 Flow same as for infinite span airfoil at angle of yaw $\pi/2 - \delta_2$
II Conical Field
III Free Stream

FIG. 2
FLOW FOR SWEPT-BACK LEADING EDGE

Boundary conditions must also be given over that part of the wing which lies inside the Mach cone. The velocity component normal to the wing must have the same value as on the rest of the wing, because of the condition that there be no flow through the wing. The boundary condition for w is that the normal derivative of w be zero on the wing. This follows from the requirement of irrotationality (implicit in the use of the potential Φ), so that

$$\frac{\partial w}{\partial y} = \frac{\partial v}{\partial z}$$

and the condition that v is constant on the wing. The fact that the wing does not lie exactly in the plane y = 0 is neglected; this has no effect on the first order perturbation. This simplification is made throughout, so that the angle of attack enters only in the boundary values and not in the position of the boundaries.

Rectangular Wing

The problem of a plane rectangular wing was successfully solved by Busemann (1), by essentially the method employed here. Schlichting (4) had previously considered the same problem by a different method, and obtained a false result because of an analytical error. When this error is corrected, Schlichting's method becomes consistent with the conical field method, not only for rectangular wings, but also for the raked wings considered in the next section. (Raked wings were not treated by either of these authors, but their methods are easily extended to this case.)

Attention may be confined to one end of the wing. The origin of coordinates is taken at the end of the leading edge. The positive x - axis is directed spanwise away from the wing. The y - axis is normal to the wing; the direction of the positive y - axis may be regarded as "upward". The positive z - axis is in the direction of flow (the coordinates being such that the wing is considered to be at rest with the air flowing past it). The velocity of the incident flow is W , the angle of attack α , and the Mach angle $\mu = \sin^{-1} 1/M$. For a wing of infinite span, the usual two-dimensional theory* gives

$$w = \alpha W \tan \mu \equiv w_\infty$$

above the wing and

$$w = -w_\infty$$

below the wing. In terms of the polar variables R and φ , the boundary conditions for w are:

$$\frac{\partial w}{\partial \varphi} = 0 \quad \text{for} \quad \varphi = \pm \pi, \quad 0 < R < A$$

$$w = +w_\infty \quad \text{for} \quad \frac{\pi}{2} < \varphi < \pi, \quad R = A$$

$$w = 0 \quad \text{for} \quad -\frac{\pi}{2} < \varphi < +\frac{\pi}{2}, \quad R = A$$

$$w = -w_\infty \quad \text{for} \quad -\pi < \varphi < -\frac{\pi}{2}, \quad R = A$$

These boundary conditions of course apply equally well in the (r, φ) plane, replacing the circle R = A by the circle r = 1. To find w, it is only necessary to solve Laplace's equation in the polar coordinates r and φ with the above boundary conditions. The solution may be constructed by the usual methods from the particular solutions $r^s \sin s\varphi$. From the first boundary condition it is seen that S must be half of an odd integer. The most general function which is harmonic in the cut circle, which satisfies the required conditions along the cut, and which is an odd function of φ (as required by the symmetry of the boundary conditions) is

$$w = \sum_{n=0}^{\infty} A_n r^{n+1/2} \sin(n+1/2)\varphi$$

* See, for example, von Mises and Friedrichs, Fluid Dynamics, p. 237, Brown University, 1942.

This is not the conventional Fourier series for a function which is periodic with period 2π ; however, it is useful to notice that the series is periodic with period 4π . This suggests the extension of the problem to a two-sheeted Riemann surface by analytic continuation across the cut. It is convenient to retain the symmetry by considering φ to range from -2π to $+2\pi$;

then the boundary values on the arcs in the "lower" sheet of the Riemann surface (that is, $-2\pi < \varphi < -\pi$ and $\pi < \varphi < 2\pi$)

are to be assigned in such a way that the even harmonics, which cannot appear in the series for w drop out. This is done by assigning boundary values in the lower sheet which are the negative of the values at corresponding points of the upper ("physical") sheet. Then

$$A_n = -\frac{w_\infty}{2\pi}\int_{-3\pi/2}^{-\pi/2} \sin(n+\tfrac{1}{2})\,\varphi\, d\varphi + \frac{w_\infty}{2\pi}\int_{\pi/2}^{3\pi/2} \sin(n+\tfrac{1}{2})\,\varphi\, d\varphi$$

$$= \frac{(-1)^n 4 w_\infty}{\pi}\,\frac{\sin(n+\tfrac{1}{2})\tfrac{\pi}{2}}{2n+1}$$

Using the symbol R to indicate "real part of", the Fourier series for w may be written as

$$w = \frac{2w_\infty}{\pi}\,\mathcal{R}\sum_{n=0}^{\infty}(-1)^n\,\frac{\left[re^{i(\varphi-\pi/2)}\right]^{n+1/2} - \left[re^{i(\varphi+\pi/2)}\right]^{n+1/2}}{2n+1}$$

$$= \frac{2w_\infty}{\pi}\,\mathcal{R}\left\{\tan^{-1}\left[\sqrt{r}\,e^{i(\varphi/2-\pi/4)}\right] - \tan^{-1}\left[\sqrt{r}\,e^{i(\varphi/2+\pi/4)}\right]\right\}$$

$$\frac{w}{w_\infty} = \frac{1}{\pi}\tan^{-1}\frac{2\sqrt{r}\cos(\varphi/2-\pi/4)}{1-r} - \frac{1}{\pi}\tan^{-1}\frac{2\sqrt{r}\cos(\varphi/2+\pi/4)}{1-r} \tag{4}$$

For $\varphi = +\pi$, $\dfrac{w}{w_\infty} = \dfrac{2}{\pi}\tan^{-1}\dfrac{\sqrt{2r}}{1-r} = \dfrac{2}{\pi}\sin^{-1}\sqrt{\dfrac{2r}{1+r^2}}$

$$= \frac{2}{\pi}\sin^{-1}\sqrt{\frac{R}{A}} \tag{5}$$

$$= \frac{1}{2} + \frac{1}{\pi}\sin^{-1}\left(2\frac{R}{A}-1\right) \tag{5'}$$

On the lower surface of the wing

$$(\varphi = -\pi)$$

w is merely changed in sign. The right member of Eq. (5) or (5') is shown as a function of R/A in Fig. 3. From the form (5'), it is clear that the curve is symmetric with respect to the point (1/2, 1/2), so that the average value of w along any spanwise line from R = 0 to R = A is just $w_\infty/2$. The triangle cut off by the Mach cone contributes just one half as much to the lift as an equal area located in the region where two-dimensional calculations are valid. (It will be seen in the next section that the same simple result holds for raked wings with leading and trailing edges perpendicular to the flow.) Formulae for lift coefficient and center of pressure are now easily obtained. If $C_{L\infty}$ is the lift coefficient for a plane wing of infinite span, and C_L the lift coefficient for a rectangular wing of total span s and chord c,

$$\frac{C_L}{C_{L\infty}} = 1 - \frac{1}{2}\frac{c}{s}\tan\mu \tag{6}$$

The center of pressure is located at a distance back from the leading edge expressed by

$$z = \frac{c}{2}\,\frac{1 - \frac{2}{3}\,c/s\,\tan\mu}{1 - \frac{1}{2}\,c/s\,\tan\mu} \tag{7}$$

The above discussion tacitly assumes that the two Mach cones from the tips do not intersect on the wing. However, this restriction is seen to be unnecessary. If Φ_1 is the (disturbance) potential inside one of the cones, Φ_2 the potential inside the other cone, and Φ_∞ the potential for a wing of infinite span with leading edge perpendicular to the stream, then in the region common to the two cones the potential is $\Phi = \Phi_1 + \Phi_2 - \Phi_\infty$. To verify this, it may be noted that Φ_1, Φ_2 and Φ_∞ are solutions of the Prandtl-Glauert Eq. (1), and since that equation is linear, Φ is a solution as well. Also Φ and its first derivatives (u, v, w) are continuous across the conical surfaces bounding the region in question. It may be said that the "tip effects" from the two tips are additive, since the equation defining Φ may be written

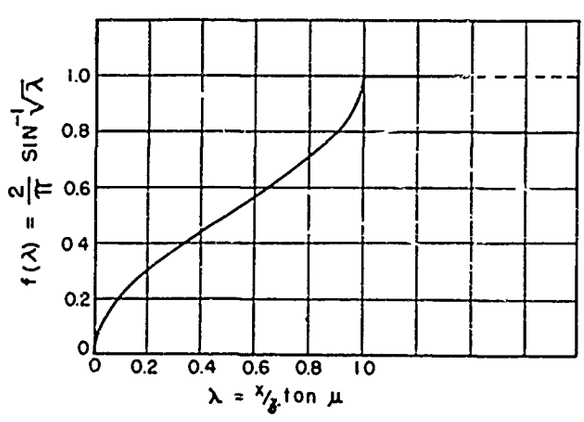

λ is the fractional distance inboard, spanwise, from the wing tip to the Mach cone.

FIG. 3

PRESSURE DISTRIBUTION ALONG SPAN FOR RECTANGULAR WING OR FOR RAKED-BACK RECTANGULAR WING WITH $|\varepsilon| < \mu$

$$(\Phi_\infty - \Phi) = (\Phi_\infty - \Phi_1) + (\Phi_\infty - \Phi_2)$$

It should be noted that the flow in the region in question is not a "conical field". The combination of the two conical fields with different vertices is never a conical field, although it approaches a conical field asymptotically downstream.

This solution is limited by the condition that the Mach cone from one tip should not intersect the other end of the wing. If this happens a further alteration is needed to satisfy boundary conditions at the edge, and the difficulty of the problem is increased enormously.

Since overlapping "tip effects" are additive, the lift coefficient and center of pressure are easily calculable as long as the Mach cone from one wing tip does not cut the other wing tip. After calculation, it is found that Eqs. (6) and (7) also hold for the overlapping case. It may be noticed that as the quantity $\frac{c}{2}\tan\mu$ increases from 0 to 1 (the highest value for which the solution applies), the ratio $C_L/C_{L\infty}$ decreases from 1 to 1/2, and the center of pressure moves from C/2 forward to C/3.

Raked Wing

The following treatment applies to wings with a positive rake angle δ, defined in such a way that the leading edge is greater than the trailing edge. If $\delta > \mu$, the problem is quite simple. The pressure on the wing is uniform and is to be calculated from two-dimensional theory. This is seen by considering the wing as carved out of an infinite span wing, which only involves removing portions whose domain of influence does not contain any part of the final trapezoidal wing.

If $0 < \delta < \mu$, the boundary conditions differ from the previously considered special case of the rectangular wing only in that the "cut" or radial line on which $\partial w/\partial n = 0$ (and across which w is necessarily discontinuous) does not extend as far as the coordinate origin. The cut along $\varphi = \pm\pi$ in the (R, φ) plane runs from $R = A = \tan\mu$ to $R = +\tan\delta$. In the (r, φ) plane the cut is still on the ray $\varphi = \pm\pi$ and runs from r = 1 to

$$r = +\frac{\tan\mu}{\tan\delta} - \sqrt{\left(\frac{\tan\mu}{\tan\delta}\right)^2 - 1} \equiv r_0$$

The new problem may be solved by finding a conformal transformation which carries it back to the already solved problem of the rectangular wing. To do this it is advantageous to map both the new and the old problem onto a half-plane. Letting $\varepsilon = re^{i\varphi}$, the transformation

$$\varepsilon = \xi - \sqrt{\xi^2 - 1} \qquad \text{or} \qquad \xi = \xi_1 + i\xi_2 = \frac{1+\varepsilon^2}{2\varepsilon}$$

maps the upper half of the circle $|\varepsilon| \leq 1$ onto the upper half plane $\xi_2 \geq 0$. The transformed boundary conditions relate to the real axis $\xi_2 = 0$

$$w = 0 \quad \text{for } \xi_1 > 0$$

$$w = 0 \quad \text{for } \xi_1 < \frac{1+r_0^2}{2r_0} = -\frac{\tan\mu}{\tan\delta} \equiv \xi_0$$

$$w = w_\infty \quad \text{for } -1 < \xi_1 < 0$$

$$\frac{\partial w}{\partial n} = 0 \quad \text{for } \xi_0 < \xi_1 < -1$$

The ultimate objective is to find a transformation which connects the ε plane with the $\varepsilon'(=r'e^{i\varphi'})$ plane corresponding to a fictitious rectangular wing. The ε' plane is mapped onto the ξ' plane by the same transformation which connects ε and ξ. The boundary conditions in the ξ' plane are obtained from those in the ξ plane by setting $\xi_0 = -\infty$

The transformation which carries the ξ plane into the ξ' plane is now clear; it must be the homographic transformation which carries the points

$$(\xi_0, -1, 0)$$

into

$$(\infty, -1, 0)$$

This is easily found to be

$$\xi' = \frac{(\xi_0+1)\xi}{\xi_0-\xi}$$

or

$$\xi = \frac{\xi_0\xi'}{\xi'+\xi_0+1}$$

The transformation from the ε' plane to the ε plane is now known, since

$$\varepsilon' = \xi' - \sqrt{\xi'^2-1} \qquad \xi' = \frac{(\xi_0+1)\xi}{\xi_0-\xi} \qquad \xi = \frac{1+\varepsilon^2}{2\varepsilon}$$

By eliminating ξ' and ξ it is possible to obtain ε' as a function of ε. In the plane of the wing, where $\varphi = 0$ or π and $\xi = A/Re^{i\varphi}$ the result simplifies to

$$\frac{R'e^{i\varphi'}}{A} = \frac{Re^{i\varphi}+R_o}{A-R_o} \qquad \varphi', \varphi = 0 \text{ or } \pi$$

Here R_o, φ_o are the polar coordinates of the edge of the wing; φ_o is 0 or π according as the rake is positive or negative. On the surface of the wings

$$\frac{R'}{A} = \frac{R-R_o}{A-R_o} \qquad \varphi' = \varphi = \pi$$

As R' goes from 0 to A, R goes from R_o to A, and the dependence of R' on R is linear. Thus the lift for a raked wing also varies according to

$$f(\lambda) = \frac{2}{\pi} \sin^{-1} \sqrt{\lambda}$$

where $\lambda = R'/A$ is the fraction of the spanwise distance from the edge of the wing to the Mach cone. The function $f(\lambda)$ is shown graphically in Fig. 3. Since it is now known that the spanwise average of lift from tip to cone is just one-half of the two-dimensional value, it is easy to derive formulae for lift coefficient and center of pressure. These formulae hold also if the Mach cones overlap on the wing without cutting the opposite wingtip. In other words, the formulae hold for $\frac{c}{s} \tan\mu \leq 1$, where s is the mean span, or average of the span at the leading and trailing edges.

$$\frac{C_L}{C_{L_\infty}} = 1 - \frac{1}{2}\frac{c}{s}\left\{\tan\mu - \frac{\tan\delta_1 + \tan\delta_2}{2}\right\} \tag{8}$$

$$= 1 - \frac{1}{2}\frac{c}{s}\tan\mu + \frac{S_L - S_T}{4s} \tag{8'}$$

S_L and S_T are the spans at the leading and trailing edges respectively. The center of pressure is located at the following distances behind the leading edge:

$$z = \frac{c}{2}\,\frac{1 - \frac{2}{3}\,c/s \tan\mu + \frac{1}{3}\,c/s\,\frac{\tan\delta_1 + \tan\delta_2}{2}}{1 - \frac{1}{2}\,c/s \tan\mu + \frac{1}{2}\,c/s\,\frac{\tan\delta_1 + \tan\delta_2}{2}} \tag{9}$$

It may be well to repeat at this point that these results hold only for positive rake angles ($S_L > S_T$).

Bent Leading Edge

A problem of considerable importance is illustrated in Fig. 2. The angles δ_1 and δ_2 are not necessarily acute angles, as in the case drawn, but each is assumed to lie in the range $\mu < \delta < \pi - \mu$. To simplify the immediate discussion it is assumed that the angle of the leading edge points upstream, so that $\delta_1 + \delta_2 < \pi$; it is shown later that the formulae obtained are valid without this restriction. Evidently the wing separates the problem into two parts which may be treated independently. Attention may be confined to the upper half, since the solution for the lower half differs only in sign. The points on the circle for which $\varphi = \beta_1$, and $\varphi = \pi - \beta_2$ mark the tangency of the plane Mach waves from the leading edge with the Mach cone. By elementary geometry,

$$\cos \beta_1 = \tan \mu / \tan \delta_1$$
$$\cos \beta_2 = \tan \mu / \tan \delta_2$$

From a consideration of the "domains of influence", see (Fig. 2) it is seen that the flow in the regions I_1, I_2, III is as indicated in the legend of Fig. 2. As before, the normal derivative of w vanishes on the wing. All three components of perturbation velocity vanish on the arc $\beta_1 < \varphi < \pi - \beta_2$; on the other two arcs the boundary conditions are to be obtained from the essentially two-dimensional problem of an infinite span airfoil at an angle of yaw, to which we now turn.

Let δ be the angle between the main stream direction and the leading edge of an airfoil of infinite span, so that $\pi/2 - \delta$ is the angle of yaw. It is assumed that $\mu < \delta < \pi - \mu$. The uniform flow W may be considered as a superposition of a uniform flow at velocity W cos δ parallel to the leading edge, giving rise to no perturbation, and a flow perpendicular to the leading edge at velocity $W_1 = W \sin \delta$ and effective Mach number $M_1 = M \sin \delta$. The effective angle of attack (α_1) for this second flow is measured in a plane perpendicular to the leading edge; it is related to the streamwise angle of attack (α), measured in a plane containing the stream direction and perpendicular to the plane of the wing for zero angle of attack, by the formula

$$\tan \alpha = \tan \alpha_1 \sin \delta$$

Within the limits of validity of the linear theory we need not distinguish between the angle of attack and its tangent, so that

$$\alpha = \alpha_1 \sin \delta$$

For a plane airfoil of infinite span and not yawed, the streamwise component (w) of perturbation velocity is

$$w = \alpha W \tan \mu = \frac{\alpha W}{\sqrt{M^2 - 1}} \equiv w_\infty$$

To obtain the chordwise component of perturbation velocity for an airfoil at an angle of yaw $\pi/2 - \delta$, replace α, W and M by α_1, W_1 and M_1. The streamwise component of perturbation velocity follows from multiplication by $\sin\delta$:

$$w = \frac{\alpha_1 W_1}{\sqrt{M_1^2 - 1}} \sin\delta = \frac{\alpha W \sin\delta}{\sqrt{M^2 \sin^2\delta - 1}} \tag{10}$$

or

$$w = \frac{w_\infty}{\sin\beta}$$

where, as before, $\cos\beta = \tan\mu / \tan\delta$

The boundary conditions for the remaining two arcs of the upper semicircle are

$$w = \frac{w_\infty}{\sin\beta_1} \equiv K_1 \quad \text{for } 0 < \varphi < \beta_1$$

and

$$w = \frac{w_\infty}{\sin\beta_2} \equiv K_2 \quad \text{for } \pi - \beta_2 < \varphi < \pi$$

The potential problem which is now uniquely determined in the upper semicircle may be written out immediately as a Fourier series. This is a cosine series only, because of the condition that $\partial w/\partial n = 0$ for $\varphi = 0$ and for for $\varphi = \pi$.

$$\begin{aligned} w &= \frac{\beta_1 K_1 + \beta_2 K_2}{\pi} + \frac{2}{\pi}\sum_{n=1}^{\infty} r^n \cos n\varphi \left\{ K_1 \int_0^{\beta_1} \cos nu \cdot du + K_2 \int_{\pi-\beta_2}^{\pi} \cos nu \, du \right\} \\ &= \frac{\beta_1 K_1 + \beta_2 K_2}{\pi} + \frac{K_1}{\pi}\left\{ \tan^{-1}\frac{r\sin(\varphi+\beta_1)}{1 - r\cos(\varphi+\beta_1)} - \tan^{-1}\frac{r\sin(\varphi-\beta_1)}{1 - r\cos(\varphi-\beta_1)} \right. \\ &\qquad \left. - \frac{K_2}{\pi}\left\{ \tan^{-1}\frac{r\sin(\varphi+\beta_2)}{1 + r\cos(\varphi+\beta_2)} - \tan^{-1}\frac{r\sin(\varphi-\beta_2)}{1 + r\cos(\varphi-\beta_2)} \right\} \right. \end{aligned} \tag{11}$$

In Eq. (11) each inverse tangent is restricted to its principal values ($-\pi/2$ to $+\pi/2$). The details of this summation are not much different than for the case of the rectangular wing, and need not be dwelt upon here.

In the symmetrical case $\delta_1 = \delta_2$, the expression (11) for w on the wing ($\varphi = 0, \pi$) simplifies to

$$w = \frac{2K}{\pi}\left\{\beta + \tan^{-1}\frac{r^2 \sin 2\beta}{1-r^2\cos 2\beta}\right\}$$

$$= \frac{2}{\pi}\frac{w_\infty}{\sin\beta}\tan^{-1}\frac{\tan\beta}{\sqrt{1-R^2/A^2}} \qquad (12)$$

Returning to the general case (δ_1 and δ_2 not necessarily equal) we seek the average value of w along the segment of a spanwise line (i.e., perpendicular to the stream) cut off by the Mach cone. It is necessary to evaluate integrals such as

$$\frac{1}{A}\int_0^A \tan^{-1}\frac{r\sin\gamma}{1-r\cos\gamma}\,dR$$

Since $R/A = 2t/1+t^2$, integration by parts leads to

$$\frac{1}{A}\int_0^A \tan^{-1}\frac{r\sin\gamma}{1-r\cos\gamma}\,dR = \frac{\pi}{4}\tan\gamma + (1-\sec\gamma)\frac{\pi-\gamma}{2}$$

where $0<\gamma<2\pi$. Using this result it is found that the average value sought is

$$\bar{w} = \frac{K_1}{2}(1+\tan\beta_1-\sec\beta_1) + \frac{K_2}{2}(1+\tan\beta_2-\sec\beta_2) \qquad (13)$$

Case of Intersecting Envelopes

For treating forward sweep or dihedral, it is necessary to discuss the plane waves from the leading edge in more detail. On one side there is a weak shock wave and on the other side a weak expansion wave; however, in the linear theory the distinction between shock waves and rarefaction waves disappears.* Both are regarded merely as surfaces of discontinuity, which can occur only across the envelope of Mach cones with

* It is this fact which makes possible the usual two-dimensional linear and second order calculations, in which the pressure is determined by local conditions and does not depend on the history of the flow up to that point. The entropy increase is of the third order in the perturbation velocity components, whereas the linear theory retains only the first order.

vertex on the leading edge. As the simplest example, Fig. 4 shows a section perpendicular to the main stream for the case of a wing with dihedral and with the leading edge perpendicular to the main stream. The situation for a plane wing with forward sweep would differ only in that the trace LMN of the wing in Fig. 4 would be straight, and overlapping of the plane waves would occur over the bottom arc as well as the top.

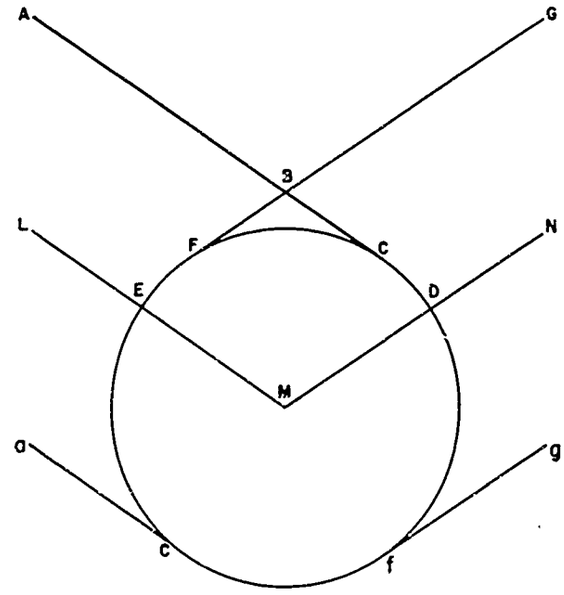

In Case drawn Leading Edge is Perpendicular to Stream

FIG. 4

WING WITH DIHEDRAL, SECTION BY PLANE PERPENDICULAR TO STREAM

The envelope of all Mach cones with vertex on LM consists of two half planes with traces AC and ac. Similarly the Mach cones with vertex on MN give rise to the envelope represented by FG and fg. It is important to notice that no arc of the circle is a part of either envelope. Within the bounds of the linear theory, shock waves or rarefaction waves intersect without mutual interference, and the perturbations caused by each are additive. In the region GBCDN the flow is uniform; in the region ABFEL there is another uniform flow; in the region between FBC and the circle the flow is also uniform, since the components of the perturbation velocity are obtained by addition of the components of perturbation velocity for the other two uniform flows. This completes the specification of the boundary conditions for the upper part of the circle. When dealing with u, v, or w, the function sought assumes a constant value of EF, another constant value on CD (both of these constants obtainable from two-dimensional theory), and a constant value on the arc FC, namely the sum of the other two constants. The boundary conditions for the lower part of Fig. 4 present nothing new; u, v, and w take on calculable (constant) values on the arcs Ec and fD, and the value zero on the arc cf.

Review of the problem illustrated by Fig. 2 now shows that the analysis given holds also for the case of a wing with forward sweep, that is, a wing with the angle pointing downstream. The only difference is a slight modification of Fig. 2.

Trapezoidal Wing

The lift coefficient and center of pressure for the symmetrical trapezoidal wing shown in Fig. 5 may now be studied. The leading and trailing edges are perpendicular to the main stream, and the tip angle (δ) is greater than the Mach angle. Since the leading edge is perpendicular to the stream, $\delta_2 = \beta_2 = \pi/2$ and the subscript may be dropped from δ_1 and β_1. In the region I,

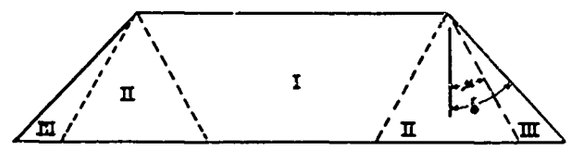

FIG. 5

$$\frac{\overline{w}}{w_\infty} = 1.$$

In the region II, the average w is found from Eq. (13):

$$\frac{\overline{w}}{w_\infty} = \frac{1}{2} + \frac{1 + \tan\beta - \sec\beta}{2\sin\beta}$$

In the region III,

$$\frac{\overline{w}}{w_\infty} = \csc\beta$$

On taking the average of these quantities, weighted according to the area in which each applies, it is found that

$$\frac{C_L}{C_{L_\infty}} = 1. \tag{14}$$

Similarly the center of pressure is found to lie behind the leading edge by the distance

$$z = \frac{c}{2}\left\{1 + \frac{1}{3}\frac{c}{s}\tan\delta\right\} \tag{15}$$

Thus in this case <u>the lift coefficient and center of pressure are the same as if the wing were subject to the uniform lift distribution of an infinite span airfoil</u>. The actual lift is not uniform; in the region I the lift is that of an infinite span airfoil; in the region II the lift is less, and in the region III the lift is greater by just enough to compensate for the decreased lift in II. As an example, Fig. 6 shows the spanwise pressure distribution for the case $\delta = 45°, \mu = 30°$ ($M = 2$).

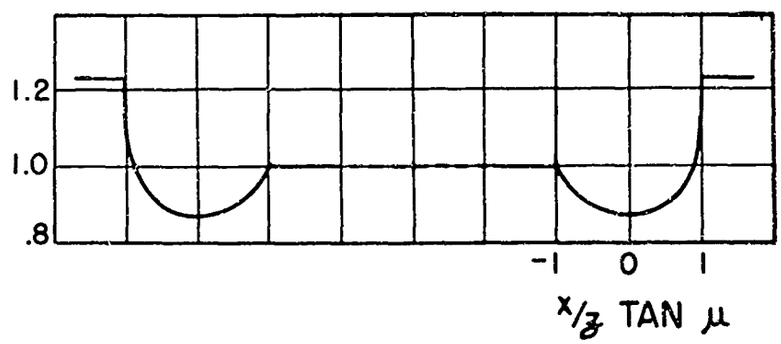

FIG. 6

PRESSURE DISTRIBUTION ALONG A SPAN LINE FOR TRAPEZOID WITH $\delta = 45°$, $\mu = 30°$, $M = 2$

(SEE FIG. 5)

General Symmetrical Quadrilateral

The case of a quadrilateral which is symmetrical about a diagonal, that diagonal being parallel to the stream is considered here. The semi-vertex angles at the nose and tail, say δ and δ_1 respectively, are not necessarily acute angles (see Fig. 8 for the various possibilities); it is assumed only that each lies in the range $\mu < \delta < \pi - \mu$. It is, of course, necessary that $\delta + \delta_1 < \pi$.

The forward pointing triangle is a special case, $\delta_1 = \pi/2$. It is also a special case of the trapezoid; setting $S_L = 0$ or $S = c \tan \delta$ in Eqs. (14) and (15) leads to

$$\left.\begin{aligned} C_L/C_{L_\infty} &= 1 \\ z &= 2c/3 \end{aligned}\right\} \qquad (16)$$

Here c is the distance from the vertex to the trailing edge. Fig. 7 shows the pressure distribution spanwise for the case $\delta = 45°$, $\mu = 30°$ $(M = 2)$. Fig. 7 is applicable to any other case for which $\tan \delta = \sqrt{3} \tan \mu$ by a uniform change of scale.

For the more general quadrilateral of Fig. 8, the lift distribution is shown by Eq. (12) in connection with Eq. (3); the calculation of lift and

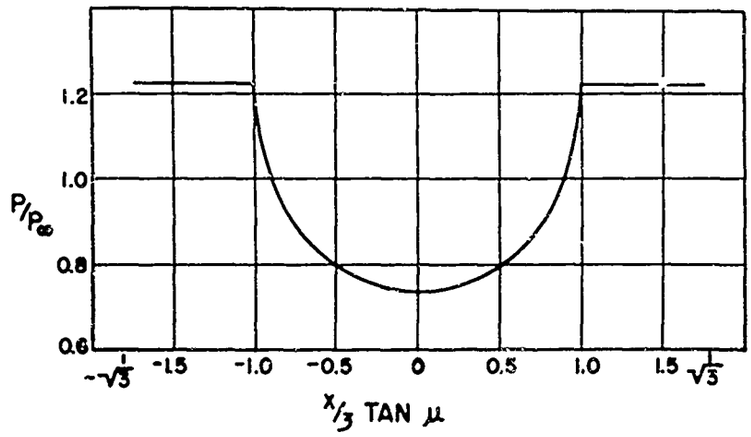

Semi-vertex angle $\delta = 45°$
Mach angle $\mu = 30°$
Mach number $M = 2$

FIG. 7

PRESSURE DISTRIBUTION
ALONG SPAN LINE FOR
FORWARD POINTING TRIANGLE

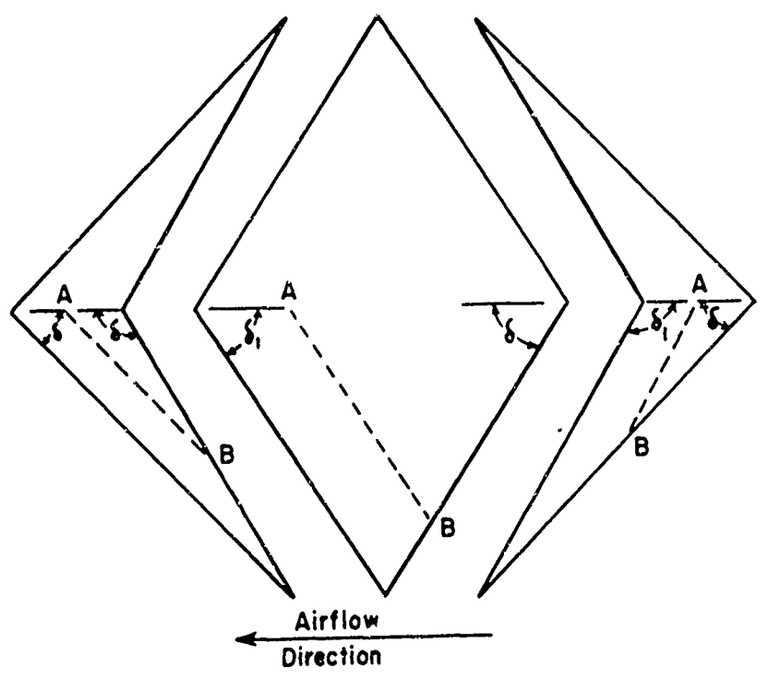

FIG. 8

center of pressure involves a tedious integration. The most convenient procedure for finding the average pressure over the wing is to integrate along any line (AB in Fig. 8) parallel to the trailing edge on one side. This gives for the average value of w, by Eq. (12)

$$\overline{w} = \frac{w_\infty}{\sin\beta} \frac{\int_0^{t_1} \frac{2}{\pi} \tan^{-1} \frac{\tan\beta}{\sqrt{1-\lambda^2}}\, dt + \int_{t_1}^{t_2} dt}{\int_0^{t_2} dt}$$

$$\text{where } \lambda = \frac{R}{A} \qquad t = \frac{\lambda \sec\delta_1}{\lambda + \sec\beta_1}$$

$$t_1 = t\Big]_{\lambda=1} = \frac{\sin\mu}{\sin(\mu+\delta_1)} \qquad t_2 = t\Big]_{\lambda=\sec\beta} = \frac{\sin\delta}{\sin(\delta+\delta_1)}$$

The integration leads eventually to

$$\frac{C_L}{C_{L\infty}} = \frac{\overline{w}}{w_\infty} = \frac{2}{\pi} \frac{\beta_1 \sin 2\beta - \beta \sin 2\beta_1}{\sin\beta_1 \sin 2\beta - \sin\beta \sin 2\beta_1} \tag{17}$$

The angles β and β_1 are, of course, to be measured in radians. This expression for $C_L/C_{L\infty}$ is symmetric in the two angles β and β_1, and therefore <u>is unchanged by interchanging</u> δ and δ_1

The center of pressure is at

$$z = \frac{2c}{3}(1 - \bar{t}\cos\delta_1) \tag{18}$$

where $\bar{t}$ is the weighted average of t along AB, with weights proportional to the pressure. It is found that

$$\bar{t}\cos\delta_1 = \frac{\int_0^{t_1} t \cdot \frac{2}{\pi} \tan^{-1} \frac{\tan\beta}{\sqrt{1-\lambda^2}}\, dt + \int_{t_1}^{t_2} t\, dt}{\int_0^{t_1} \frac{2}{\pi} \tan^{-1} \frac{\tan\beta}{\sqrt{1-\lambda^2}}\, dt + \int_{t_1}^{t_2} dt} \cos\delta_1$$

$$= \frac{1}{2} \frac{\cos^2\beta_1 + \cos^2\beta}{\cos^2\beta_1 - \cos^2\beta} + \frac{\sin 2\beta}{2\sin^2\beta_1} \cdot \frac{\sin 2\beta_1 - 2\beta_1 \cos 2\beta_1}{2\beta_1 \sin 2\beta - 2\beta \sin 2\beta_1} \tag{19}$$

These formulae contain as special cases the forward pointing triangle ($\beta_1 = \pi/2$) and the backward pointing triangle ($\beta = \pi/2$). For these triangles, the invariance of lift coefficient (and in this particular case, the center of pressure also) with respect to reversal of the flow direction may be easily verified. It has already been shown that lift coefficient and center of pressure for the forward pointing triangle are the same as if the pressure were uniform (which it is not; cf. Fig. 7). For the backward pointing triangle the pressure is uniform. Reversal of direction of flow causes a radical change in pressure distribution even though it does not alter the lift coefficient for these quadrilateral wings.

Another special case of interest is the diamond ($\delta_1 = \delta$, $\beta_1 = \beta$). In this case Eqs. (18) and (19) reduce to

$$\frac{C_L}{C_{L_\infty}} = \frac{\sin 2\beta - 2\beta\cos 2\beta}{\pi \sin^3\beta} \tag{20}$$

$$\frac{z}{c} = \frac{1 - \frac{1}{3}\,\frac{2\beta \sin^2 2\beta}{\sin 2\beta - 2\beta\cos 2\beta}}{1 - \cos 2\beta} \tag{21}$$

Using Eqs. (20) and (21), the lift coefficient and center of pressure for a diamond have been evaluated and are presented in the following table. It is seen at once that the property of invariance under reversal of flow direction, which was found to hold for C_L, does not in general apply to the center of pressure. If such were the case the center of pressure of the diamond would necessarily be at $z = c/2$ From Table I it is seen that the center of pressure of a diamond actually lies forward of the midpoint, though never forward of $7c/15$ as long as $\delta > \mu$

Table I.

β	0°	10°	20°	30°	40°
C_L/C_{L_∞}	.8488	.8511	.8592	.8720	.8897
z/c	.4667	.4671	.4685	.4709	.4743
$\tan\delta/\tan\mu$	1.000	1.015	1.064	1.155	1.305
β	50°	60°	70°	80°	90°
C_L/C_L	.9120	.9376	.9646	.9885	1.000
z/c	.4788	.4842	.4905	.4966	.5000
$\tan\delta/\tan\mu$	1.556	2.000	2.924	5.759	∞

Wing With Dihedral

The case of a wing with dihedral, which may be combined with forward or backward sweep at the dihedral point, is reducible by a conformal transformation to the case of a simple bend in the leading edge of a flat wing. In Fig. 9, the angle $\varphi = 0$ has been taken in the wing (with no loss of generality). Let γ be the radian measure of the arc of the circle subtended by the wing. The part of the circle not drawn refers to an independent problem of the same type, with a different γ. The angles β_1 and β_2 have the same meaning as in the plane case. In the case shown, $\beta_1 + \beta_2 < \gamma$ (which incidentally corresponds to considerable sweepback in this case), but this condition is not essential, and is assumed here merely to simplify the drawing.

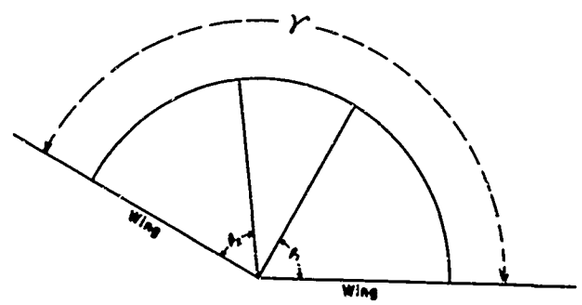

FIG. 9

The potential problem to be solved in the t, φ plane involves the following boundary conditions:

$$\frac{\partial w}{\partial \varphi} = 0 \quad \text{for} \quad \varphi = 0 \text{ or } \varphi = \gamma, \quad 0 < r < 1$$

$$w = K_1 \quad \text{for} \quad 0 < \varphi < \beta_1, \quad r = 1$$

$$w = K_2 \quad \text{for} \quad \gamma - \beta_2 < \varphi < \gamma, \quad r = 1$$

$$w = 0 \quad \text{for} \quad \beta_1 < \varphi < \gamma - \beta_2, \quad r = 1$$

The transformation $\mathcal{E}' = \mathcal{E}^{\pi/\gamma}$ maps the relevant part of the unit circle in the $\mathcal{E} = r e^{i\varphi}$ plane into the upper half of the unit circle in the $\mathcal{E}' = r' e^{i\varphi'}$ plane. It is clear that w is given by Eq. (11), with r replaced by $r^{\pi/\gamma}$, and every angle (β_1, β_2 and φ) multiplied by π/γ

It remains to specify $\beta_1, \beta_2, K_1, K_2$ in terms of the geometry of the wing. As in the plane case,

$$\cos\beta_1 = \frac{\tan\mu}{\tan\delta_1} \quad , \quad \cos\beta_2 = \frac{\tan\mu}{\tan\delta_2}$$

where δ_1 and δ_2 are the angles from the main stream direction to the leading edge. The boundaryvalues K_1 and K_2 are given by the same expression as for a plane wing, except that the angle of attack is now, in general, different for each plane of the wing. Writing α_1 and α_2 for these "local" angles of attack, one find that

$$K_1 = \frac{\alpha_1 W \tan\mu}{\sin\beta_1} \qquad K_2 = \frac{\alpha_2 W \tan\mu}{\sin\beta_2}$$

It is interesting to note that in the case of symmetry

$$(\delta_1 = \delta_2 \ , \ \alpha_1 = \alpha_2)$$

there is a certain dihedral, namely $\gamma = 2\beta$, for which the boundary condition is w = k over the entire arc γ, so that the flow is uniform in the whole sector.

The restriction $\beta_1 + \beta_2 < \gamma$ is seen to be non-essential as in the previous case of a bent leading edge. Also it should be pointed out that for a wing with upswept dihedral ($\gamma < \pi$ for the upper surface) the lift is decreased in magnitude.

An application of these formulae may be found in the perpendicular vane at the tip of a rectangular wing, the vane being large enough to project through the Mach cone. This may be regarded as an example of a wing with dihedral, one of the angles of attack being zero. If the vane extends both above and below the wing, the lift remains constant out to the end of the wing. If the vane is confined to either the top or the bottom of the wing, the lift decreases moving along a span line toward the wingtip; the lift at the tip is 1/3 of the lift in the central region of the wing, and the spanwise average from tip to Mach cone is found by integration to be $\left(1 - \frac{2}{3\sqrt{3}}\right)$ of the lift in the central region.

References

1. Busemann, A., Infinitesimale kegelige Überschallstromung, Schriften der deutschen Akademie der Luftfahrtforschung, Band 7, Heft 3, (1943), pp. 105-121.

2. Stewart, H. J., The Lift of a Delta Wing at Supersonic Speeds, Quarterly of Applied Mathematics, Volume IV, No. 3, (October 1946).

3. Chaplygin, S., Gas Jets, Scientific Memoirs, Moscow University, Part V, (1902). Translated from the Russian as NACA Technical Memorandum No. 1063.

4. Schlicting, H., Tragflügeltheorie bei Ueberschallgeschwindigkeit, Luftfahrtforschung 13 (1936), pp. 320-335. Translated as NACA Technical Memorandum No. 897.

I. AERODYNAMIC CHARACTERISTICS OF SOLID RECTANGULAR AIRFOILS AT SUPERSONIC SPEEDS*

by E. A. Bonney

Summary

The lift, drag, moment, and center-of-pressure characteristics of rectangular airfoils can readily be obtained for angles of attack below that at which the shock wave detaches from the leading edge of the airfoil. This report presents expressions for the above characteristics and establishes optimum values of aspect ratio, angle of attack, and lift-drag ratio for any given conditions of allowable stress, airfoil cross-sectional shape and Mach number as well as method of supporting the wing, i.e. by the entire base or on a hub.

Assumptions

It was necessary to make certain simplifying assumptions to keep the various expressions reasonably simple and yet accurate. They are as follows:

1. The change in Mach angle with positive angle of attack over an airfoil of finite thickness and aspect ratio was ignored. The angle will be higher on the lower surface and lower on the upper surface, thereby offsetting each other to a great extent.

2. The possibility of secondary tip effects originating at the point of maximum thickness of a double wedge airfoil for example was not considered.

3. Consideration of the phenomena of separation necessarily was omitted due to the lack of knowledge of this effect in supersonic flow. This factor can cause the center of pressure expressions obtained herein to be somewhat in error, particularly at high angles of attack. A study of the effects of separation is contained in reference (12).

4. A constant skin friction drag coefficient of $C_{D_f} = .00265$ per square foot of wetted area is used throughout. This is the value obtained by von Karman for a Reynolds number of about 20,000,000. It is recognized that the actual value may be considerably different than this and, inasmuch as skin friction is the predominant factor in the drag of thin airfoils, can cause a corresponding difference in the values for optimum conditions.

---

* This paper is a revision of CM-247 which was originally published as an internal memorandum of the Applied Physics Laboratory. Slight revision was necessary to complete the discussion of the subject.

5. The expression for aspect ratio correction to lift curve slope for an infinitely thin flat plate was used in deriving optimum conditions for simplification. The maximum error that could result from this assumption is about 3 per cent for practical airfoil sizes.

6. Throughout the analysis the assumption is made that

$$\sin \alpha = \alpha \text{ and}$$
$$\cos \alpha = 1$$

This will cause no sizable error for angles of attack up to 15 degrees.

Nomenclature

The following nomenclature is used throughout this paper:

b = wing semi-span

c = chord

$\mathcal{AR} = \frac{2b}{c}$ = aspect ratio

M = Mach number

$\mathcal{M} = \sqrt{M^2 - 1}$

$R = \mathcal{AR} \times \mathcal{M}$

μ = Mach angle = $\sin^{-1} \frac{1}{M} = \tan^{-1} \frac{1}{\mathcal{M}}$

p = local static pressure at any point on the airfoil

P_o = free stream static pressure

ρ_o = free stream density

V = velocity in ft/sec.

$q = \frac{\rho_o V^2}{2} = \frac{\gamma}{2} p_o M_o^2$ = free stream dynamic pressure

L = lift

$A = 2bc$ = wing area

$C_L = \frac{L}{qA}$ = lift coefficient of finite span airfoil

C_{L_o} = lift coefficient of an infinite span airfoil

D = drag

$C_D = \frac{D}{qA}$ = drag coefficient of finite span airfoil

M = moment about leading edge of wing

$C_M = \frac{M}{cqA}$ = moment coefficient about leading edge

c.p. = center of pressure measured from leading edge

C_{D_f} = skin friction drag coefficient

C_{D_F} = form drag coefficient

C_{D_W} = wave drag coefficient due to lift

K_λ = coefficient for taper in thickness

K_1 = coefficient for wing form drag

K_4 = coefficient for wing strength

$w = C_L q$ = wing loading

$K_3 = \frac{K_\lambda K_1 K_4 w}{2S}$

S = stress

s = section modulus

t_1 = wing thickness at root

t_2 = wing thickness at tip

α = angle of attack

β = semi-vertex angle of leading edge

θ = local angle between any point on the surface of the airfoil and the free stream direction

γ = ratio of specific heats

$p' = \frac{p-p_o}{q} = \frac{\Delta p}{q}$ = pressure coefficient

Subscripts

U = upper surface of airfoil

L = Lower surface

F = forward half of double wedge airfoil

R = rear half

o = free stream conditions

Discussion

A. Basic equations of lift, drag, moment, and center of pressure for infinitely thin flat plates and for airfoils, both with infinite and finite aspect ratios.

Various methods (references 4, 10, and 11) have been developed for determining the pressure on an airfoil in supersonic flow where a shock wave has formed and is attached to the leading edge. However they do not all lend themselves to convenient handling for purposes of developing expressions for lift and drag of the airfoils. The one exception to this is the Busemann "second order approximation" (see ref. 4 and 10) which is usually written as follows:

$$p/p_o = 1 + 2\gamma \operatorname{cosec} 2\mu_o\theta + \gamma \sec^2\mu_o \operatorname{cosec}^2 2\mu_o(\gamma + \cos^2 2\mu)\theta^2 \qquad (1)$$

Transforming by use of the fundamental relationships,

$$\sin\mu_o = 1/M_o \quad \tan\theta = 1/M_o \quad \cos\theta = M_o/M_o \quad \text{and} \quad q = \gamma/2\, p_o M_o^2$$

a convenient expression for $\frac{\Delta p}{q}$ is obtained as follows:

$$\frac{\Delta p}{q} = \frac{2}{\sqrt{M^2-1}}\,\theta + \frac{\gamma M^4 + (M^2-2)^2}{2(M^2-1)^2}\,\theta^2 = C_1\theta + C_2\theta^2 \qquad (2)$$

This method is found to be very accurate when compared to the theoretically correct method of "patching curves" of reference (4) two dimensional method of characteristics) with the error approaching about -2 per cent in lift, drag, and moment at about 60 per cent of the detachment angle. Above this the error increases roughly in a parabolic manner until at the detachment angle it may amount to -10 to -13 per cent, depending on the geometry of the airfoil. The angle of attack at which detachment occurs (called detachment angle) decreases with decreasing Mach number and increasing leading edge wedge angle and may be determined for any condition from reference (4). The error in center of pressure location, neglecting separation, when compared to the accurate method is negligible at any angle of attack up to detachment.

From this expression, it is possible to determine the aerodynamic characteristics of any shape of airfoil of infinite aspect ratio

and if the loss in pressure at the tips for finite aspect ratio wings is also known, then they can be found for any airfoil of any aspect ratio. For example, for any wing of infinite aspect ratio and symmetrical about its chord line, the lift coefficient can be determined simply by the inspection of equation (2) as being

$$C_L = 2C_1\alpha = \frac{4\alpha}{\sqrt{M^2-1}}$$

$$(\theta = \pm\alpha \pm \beta \text{ depending on surface})$$

The loss in pressure at the tips due to flow from the lower to the upper surface has been determined in references (2) and (8) and is shown in Fig. 1. It can be seen from this figure that the assumption of a linear loss in lift from the limit of the Mach angle to the tip is justified and that the lift inside the Mach cone will therefore be one-half of the two dimensional value for the same area.

With conditions of pressure known at every point on the airfoil, it is now possible to develop expressions for lift, drag, moment and center of pressure for any type of airfoil. These expressions are listed in Table I and are good for all airfoils that are symmetrical about both the chord line and a line perpendicular to the chord at the midpoint. Sample derivation of some of these expressions will be found in the section on "Derivations".

B. Optimum design conditions for wings of finite thickness and aspect ratio for (a) wings supported over their entire base and (b) wings supported by a hub.

In determining the optimum design conditions of aspect ratio, drag, and angle of attack for various values of allowable wing stress and type of airfoil (which establish the value of K_3), and Mach number, the methods of references (7) and (9) were used for the most part.

It should be pointed out that the problem of establishing optimum conditions is, in this paper, principally of academic interest for two reasons. First the optimum type of airfoil will not be solid, but rather of monocoque construction due to the excessive weight of a solid wing and secondly, the optimum angle of attack upon which all of the other conditions depend is different for a wing on a body than for a wing alone. Various trends can be studied however, which will be applicable regardless of these factors.

Derivations

A. In this section, the method of derivation of the expressions given in Table I for lift coefficient and center of pressure of an airfoil of finite thickness and aspect ratio will be shown. Several of the other expressions will be found in the various references (see references 1, 2, 3, and 10) although perhaps not in exactly the same form. For the sake of brevity, the double wedge section will be used in the following illustrations and the final expressions generalized by a method suggested by Busemann.

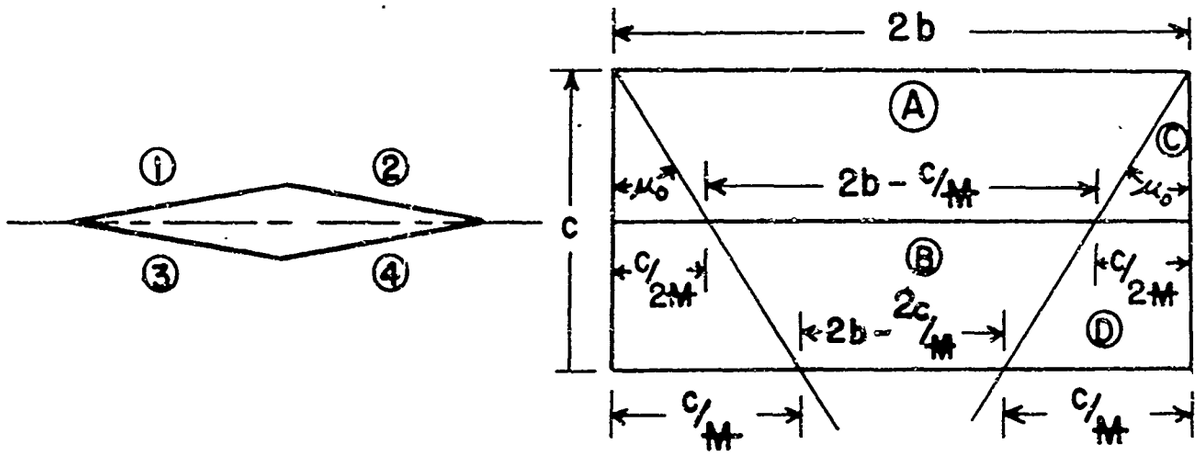

$$p' = \frac{\Delta p}{q} = C_1\theta + C_2\theta^2$$

$$\theta_1 = -\alpha + \beta$$

$$\theta_2 = -\alpha - \beta \qquad (3)$$

$$\theta_3 = \alpha + \beta$$

$$\theta_4 = \alpha - \beta$$

Therefore, the two dimensional pressure difference over the front and rear halves of the airfoil,

$$p'_{③} - p'_{①} = 2C_1\alpha + 4C_2\alpha\beta$$
$$p'_{④} - p'_{②} = 2C_1\alpha - 4C_2\alpha\beta \qquad (4)$$

Remembering that the lift in region C is equal to half of that in region A (for a like area) and likewise the lift in region D is half of that of B, then

$$C_L = \frac{(2C_1\alpha + 4C_2\alpha\beta)\left[(2b - \frac{c}{2M})\frac{c}{2} + \frac{1}{2}\times\frac{c}{2M}\times\frac{c}{2}\right] + (2C_1\alpha - 4C_2\alpha\beta)\left[(2b\frac{3c}{2M})\frac{c}{2} + \frac{1}{2}\times\frac{3c}{2M}\times\frac{c}{2}\right]}{2bc} \qquad (5)$$

Using the expressions,

$$c = \frac{2b}{AR} \text{ and } R = AR\sqrt{M^2 - 1} \tag{6}$$

the coefficient of lift becomes

$$C_L = 2C_1\alpha\left[1 - \frac{1}{2R}\left(1 - \frac{C_2\beta}{C_1}\right)\right] \tag{7}$$

This expression applies to a double wedge airfoil only. However, Busemann has pointed out that the expression can be made general for all airfoils that are symmetrical about their chord line and a line perpendicular to the chord line at the midpoint by substituting the parameter of cross-sectional area divided by the chord squared in place of the half wedge angle. Therefore for a double-wedge airfoil,

$$\frac{Acs}{c^2} = \frac{tc}{2c^2} = \frac{t}{2c} = \frac{\beta}{2} \tag{8}$$

$$\beta = \frac{2Acs}{c^2} = 2A'$$

Values of A' for various types of airfoils are noted in Table I

Therefore if

$$C_1 = \frac{2}{M} \text{ and } C_3 = \frac{2C_2}{C_1}$$

$$C_L = \frac{4\alpha}{M}\left[1 - \frac{1}{2R}(1 - C_3A')\right] \tag{9}$$

Inasmuch as the lift coefficient for infinite aspect ratio is

$$C_{L_\infty} = \frac{4\alpha}{M} \tag{10}$$

then the aspect ratio correction to 2 dimensional lift (and drag due to lift) is

$$\frac{C_L}{C_{L_\infty}} = 1 - \frac{1}{2R}(1 - C_3A') \tag{11}$$

The center of pressure is obtained by summating the center of pressure of each region times the total pressure in that region for the entire airfoil and dividing by the total pressure or lift force.

Referring again to the sketch of the airfoil.

$$\left(\frac{c.p.}{c}\right)_{Ⓐ} = \frac{1}{6}\left(\frac{2b+4b-\frac{2c}{M}}{2b+2b-\frac{c}{M}}\right) = \frac{3R-2}{12R-6} \tag{12}$$

$$\left(\frac{c.p.}{c}\right)_{Ⓑ} = \frac{1}{2}+\frac{1}{6}\left(\frac{2b-\frac{c}{M}+4b-\frac{4c}{M}}{2b-\frac{c}{M}+2b-\frac{2c}{M}}\right) = \frac{9R-14}{12R-18}$$

$$\left(\frac{c.p.}{c}\right)_{Ⓒ} = \frac{2}{3}\times\frac{1}{2} = \frac{1}{3}$$

$$\left(\frac{c.p.}{c}\right)_{Ⓓ} = \frac{1}{2}+\frac{5}{9}\times\frac{1}{2} = \frac{7}{9}$$

Area of each region

$$Ⓐ = \left(2b-\frac{c}{2M}\right)\frac{c}{2} = (2R-1)\frac{bc}{2R} \tag{13}$$

$$Ⓑ = \left(2b-\frac{3c}{2M}\right)\frac{c}{2} = (2R-3)\frac{bc}{2R}$$

$$Ⓒ = \frac{c}{2M}\,\frac{c}{2} = \frac{c^2}{4M} = \frac{bc}{2R}$$

$$Ⓓ = \frac{3c}{2M}\,\frac{c}{2} = \frac{3c^2}{4M} = 3\frac{bc}{2R}$$

Therefore the center of pressure will be, (omitting factor $\frac{bc}{2R}$ from top and bottom)

$$\frac{c.p.}{c} = \frac{(2C_1\alpha+4C_2\alpha\beta)\left[\left(\frac{3R-2}{12R-6}\right)(2R-1)+\frac{1}{3}\times\frac{1}{2}\times 1\right]+(2C_1\alpha-4C_2\alpha\beta)\left[\left(\frac{9R-14}{12R-18}\right)(2R-3)+\frac{7}{9}\times\frac{1}{2}\times 3\right]}{(2C_1\alpha+4C_2\alpha\beta)\left[2R-1+\frac{1}{2}\times 1\right]+(2C_1\alpha-4C_2\alpha\beta)\left[2R-3+\frac{1}{2}\times 3\right]}$$

$$= \frac{R-\frac{2}{3}-C_3A'(R-1)}{2R-1+C_3A'} \tag{14}$$

This expression likewise is general for all symmetrical airfoils when expressed as a function of A' rather than β .

B. For a given value of allowable stress at the root section, there will be an optimum aspect ratio which, for a given lift, will produce the least drag. At low aspect ratios, the tip loss will be great and hence the area for a given lift will be large while at high aspect ratios the thickness and hence the drag for a given stress will be large; therefore the optimum aspect ratio will be somewhere in between these two conditions and is obtained as follows:

$$D = \left[\frac{K_\lambda K_1 \tau^2}{M} + \frac{.00122\alpha^2}{M}\left(\frac{C_L}{C_{L_\infty}}\right) + C_{D_f}\right] qA \tag{15}$$

(α in degrees from this point on.)

Now for a given lift,

$$L = C_{L_\infty} q A_\infty = C_L q A \tag{16}$$

$$\therefore A = \frac{A_\infty}{\left(C_L/C_{L_\infty}\right)} \tag{17}$$

Substituting into (15)

$$D = \frac{.00122\alpha^2\left(C_L/C_{L_\infty}\right)qA_\infty}{M\left(C_L/C_{L_\infty}\right)} + \frac{K_\lambda K_1 \tau^2 q A_\infty}{M\left(C_L/C_{L_\infty}\right)} + \frac{C_{D_f} q A_\infty}{\left(C_L/C_{L_\infty}\right)} \tag{18}$$

$$\text{and } \frac{D}{qA_\infty} = \frac{.00122\,\alpha^2}{M} + \frac{K_\lambda K_1 \tau^2 + C_{D_f} M}{M\left(C_L/C_{L_\infty}\right)} \tag{19}$$

Now for a double wedge airfoil the section modulus is

$$s = \frac{ct^2}{24} = \frac{m}{S} = \frac{(wbc)b}{2S} \tag{20}$$

where the spanwise center of pressure is conservatively assumed to be at one-half the distance to the tip. From this expression the thickness ratio becomes

$$\tau^2 = \frac{3wR^2}{S} = \frac{K_4 wR^2}{S} \tag{21}$$

where K_4 is a function of the cross-sectional shape and is given in Table I for various airfoils.

Equation (19) now becomes,

$$\frac{D}{qA_\infty} = \frac{.00122\,\alpha^2}{M} + \frac{K_3 R^2 + C_{D_f} M}{M\left(C_L/C_{L_\infty}\right)} \tag{22}$$

NOTE
PAGES 32 & 33
TRANSPOSED

The parameter $K_1 \tau^2$ is plotted in Figs. 12 and 18 to show the variation in thickness ratio.

From the expressions for drag coefficient

$$C_D = \frac{.00122\alpha^2}{M}\left(1 - \frac{1}{2R}\right) + \frac{K_3 AR^b}{M} + C_{D_f}$$

and lift coefficient

$$C_L = \frac{.0698\alpha}{M}\left(1 - \frac{1}{2R}\right)$$

the drag-lift ratio becomes

$$\frac{D}{L} = .01745\alpha + \frac{K_3 AR^b + C_{D_f} M}{.0698\left(1 - \frac{1}{2R}\right)\alpha} \tag{28}$$

Differentiating with respect to α and optimizing, the optimum angle of attack becomes,

$$\alpha_{opt.} = 28.6\sqrt{\frac{2R(K_3 AR^b + C_{D_f} M)}{2R - 1}} \tag{29}$$

and the minimum drag-lift ratio becomes

$$\left(\frac{D}{L}\right)_{MIN} = .50\sqrt{\frac{2R(K_3 AR^b + C_{D_f} M)}{2R - 1}} + \frac{K_3 AR^b + C_{D_f} M}{2.0\left(\frac{2R-1}{2R}\right)\sqrt{\frac{2R(K_3 AR^b + C_{D_f} M)}{2R - 1}}}$$

$$= \sqrt{\frac{2R(K_3 AR^b + C_{D_f} M)}{2R - 1}} \tag{30}$$

and

$$\left(\frac{L}{D}\right)_{MAX} = \sqrt{\frac{2R - 1}{2R(K_3 AR^b + C_{D_f} M)}} \tag{31}$$

The interesting relation between maximum lift-drag ratio and optimum angle of attack is to be noted.

$$\alpha_{opt}\,(\text{deg.}) = \frac{28.65}{(L/D)_{MAX}} \quad \text{or} \quad \alpha_{opt}\,(\text{rad.}) = \frac{1}{2(L/D)_{MAX}} \tag{32}$$

This relation will be true for a wing alone or for a wing and body combination.

From the above expressions, the maximum lift-drag ratio and optimum angle of attack are found to be very nearly alike (within ± 3 per cent)

$$\text{where } K_3 = \frac{K_\lambda K_1 K_4 w}{S} \tag{23}$$

By a more arduous means, it may be shown that for a wing supported by a hub or shaft, the exponent of the aspect ratio will be approximately 3/2 for values of shaft diameter equal to 1 1/2 - 2 times the maximum thickness at the root. This is an approximation (because the value must again be 2 for hub diameters equal to or greater than the chord length), but it will be shown that the method of support does not affect the aerodynamic values to any great extent, but simply changes the optimum aspect and thickness ratios.

Optimizing equation (22) for aspect ratio,

$$\frac{d}{dAR}\left(\frac{K_3 AR^b + C_{D_f} M}{M\left(C_L / C_{L_\infty}\right)}\right) = 0$$

Using the expression for aspect ratio correction to lift curve slope of a flat plate for values of $R > 1$, the expression for optimum aspect ratio for a wing supported over the entire base, becomes,

$$M^3 = \frac{K_3}{C_{D_f}} R^2 (4R - 3) \tag{24}$$

and for wings supported by a hub,

$$M^{5/2} = \frac{K_3}{C_{D_f}} R^{3/2} \left(3R - \frac{5}{2}\right) \tag{25}$$

These expressions are plotted in Figs. 7 and 13 to show the variation of optimum aspect ratio with Mach number and the aerodynamic-strength parameter K_3. The corresponding expressions for values of $R < 1$ will not be derived here because, for the most part, such values are outside of the realm of practical aspect ratio - Mach number combinations.

From the development of optimum aspect ratio, it becomes apparent that, for wings supported over their entire base, that

$$K_1 \tau^2 = K_3 AR^2 \tag{26}$$

and for wings supported by a hub,

$$K_1 \tau^2 = K_3 AR^{3/2} \tag{27}$$

for both methods of support and the mean values are shown plotted in Figs. 9, 10, 15, and 16.

In order to determine the value of wing loading, w to be used in evaluating K_3, it is necessary to know either the weight and wing area or the lift coefficient and dynamic pressure. The dynamic pressure will depend on the choice of altitude and Mach number. Inasmuch as the optimum aspect ratio and angle of attack have been established, the optimum lift coefficient can readily be found and develops to be very nearly independent of the method of support and the parameter K_3. The mean value is plotted in Figs. 8 and 14.

Results

Expressions for lift, drag and moment coefficients and center of pressure for thin flat plates and airfoils of infinite and finite aspect ratio are given in table I. The lift curve slope correction and center of pressure expressions for a flat plate will be found plotted in Figs. 3 and 4. The effect of thickness on lift has not been added due to its small magnitude and the fact that it does not lend itself to a general expression for plotting, however the effect on center of pressure is quite sizable and two sample cases have been plotted in Fig. 4. The expressions of table I are exact (within limits of accuracy of the Busemann second order approximation) down to a value of R = 1. Below this value, a linear extension to 0 will be approximately correct.

The loss in lift at the tips due to flow around the tips as found in references (2) and (8) and is plotted in Fig. 1. A straight-line variation is also shown to illustrate the fact that the lift in the affected region (inside the Mach angle from the tip) is one-half of the amount for two dimensional flow for the same area.

A correction factor, K_λ for tapered (in thickness) airfoils of rectangular planform to be used in the expression for K_3 is given in Fig. 5 and the terms explained in Fig. 6. These two curves were taken directly from reference (6).

Figures 7 to 12 and 13 to 18 represent the optimum aerodynamic characteristics of symmetrical wings as a function of Mach number and K_3, the aerodynamic-strength parameter, for wings supported over their entire base and for wings supported by a hub. The similarity in magnitude of the aerodynamic coefficients for wings supported over their entire base as compared to wings supported by a hub is to be noted. Optimum aspect ratio and thickness ratio are different for the two cases, but compensate for each other so that the coefficients are nearly the same.

Conclusions

The Busemann second order approximation theory for the pressure over a two dimensional wing and the known theory for pressure loss near the tips of a finite span airfoil provide a convenient method for finding

the aerodynamic coefficients for flat plates and airfoils of finite and infinite aspect ratio at angles of attack below the detachment angle in supersonic flow. This second order theory is very accurate for angles of attack up to about sixty per cent of the detachment angle after which it departs from the exact theory at a more-or-less parabolic rate.

By a method also suggested by Busemann, it is possible to generalize the expressions to include any type of airfoil section which is symmetrical about its chord line and a line perpendicular to the chord line at its midpoint.

Decreasing the aspect ratio will decrease the lift, wave drag (herein defined as the drag due to lift), and moment coefficients and cause the center of pressure to move forward. Increasing the thickness will increase the lift and drag coefficients of airfoils of finite aspect ratio very slightly, but will decrease the moment coefficient and cause the center of pressure to move forward quite markedly for airfoils of finite and infinite aspect ratio. Increasing Mach number will either increase or decrease the coefficients depending on the magnitude of the Mach numbers being considered and the aspect ratio.

The expressions for lift check very well with available test data. The center of pressure expressions, however, make no allowance for separation effects (and other minor factors noted in items 1 and 2 under "Assumptions") and therefore will be somewhat in error, the error being a function of the angle of attack. The expressions will make it possible to determine the magnitude of the separation effects on center of pressure location however.

Using the information developed above, the optimum conditions of aspect ratio and angle of attack and the corresponding coefficients for rectangular wings supported by the entire base and supported by a hub can be determined. For a given value of the aerodynamic-strength parameter K_3, the aerodynamic coefficients are not a function of the method of support, being almost identical for either method. The aspect ratio, however, will be higher for a wing supported by a hub, the thickness ratio also being higher in general to compensate for this effect stresswise. Other effects may be noted by a study of Fig. 7 through 19.

The expressions for lift, drag and moment coefficients and center of pressure will be found in Table I. Note that an increment for skin friction has been added to the drag equations which will not appear in the derivation of the expression.

References

1. Schlichting, H. "Airfoil Theory at Supersonic Speed". NACA 897 June 1939.

2. Taunt, D. R. and Ward, G. N., S.R.E./Airflow/29. (Secret report).

3. Rae, R. W., Ward, G. N., and Orman, P. L., S.R.E./Airflow/28 TC 1/247. (Secret report)

4. Edmonson, N., Murnaghan, F. D., and Snow, R. M. "The Theory and Practice of Two Dimensional Supersonic Pressure Calculations". Bumblebee Report No. 26, Dec. 1945.

5. Porter, H. H., "Practical Airfoil Considerations" CF-119, Dec. 19, 1945 (Confidential report).

6. Porter, H. H., and Bonney, E. A., "Aspect Ratio Correction to Lift for Rectangular Wings". CM-199, Jan. 23, 1946 (Confidential report).

7. Porter, H. H., "Aspect Ratio for Minimum Drag of Rectangular Wings" CF-143, Feb. 11, 1946 (Confidential report).

8. Snow, R. M., "Finite Span Correction for Plane Airfoils at Small Angles of Attack". CM-214, Feb. 14, 1946 (Restricted report).

9. Lemmon, A. W., "Lift to Drag Ratios for Thin Rectangular Wings of Finite Aspect Ratio". CF-165, March 1, 1946 (Restricted report).

10. Lock, G. N. H., "Examples of the Applications of Busemann's Formula to Evaluate the Aerodynamic Coefficients on Supersonic Airfoils". Sept, 4, 1944 TC 1/192 (Restricted report).

11. Busemann, A. "Handbuch der Experimentalphysik Wien - Harms". Vol. 4 Pgs. 343 - 460 RTP Translation 2207.

12. Ferri, A, "Experimental Results with Airfoils Tested in the High Speed Tunnel at Guidonia". NACA TM-946.

TABLE I

SUMMARY OF AIRFOIL CHARACTERISTICS

TYPE AR	FLAT PLATE INFINITE	FLAT PLATE FINITE	AIRFOIL INFINITE	AIRFOIL FINITE
C_L	$\frac{4\alpha}{M}$	$\frac{4\alpha}{M}\left(1-\frac{1}{2R}\right)$	$\frac{4\alpha}{M}$	$\frac{4\alpha}{M}\left[1-\frac{1}{2R}\left(1-C_3A'\right)\right]$
C_D	$\frac{4\alpha^2}{M}+C_{D_f}$	$\frac{4\alpha^2}{M}\left(1-\frac{1}{2R}\right)+C_{D_f}$	$\frac{K_1\left(\frac{t}{c}\right)^2}{M}+\frac{4\alpha^2}{M}+C_{D_f}$	$\frac{K_1\left(\frac{t}{c}\right)^2}{M}+C_{D_f}+\frac{4\alpha^2}{M}\left[1-\frac{1}{2R}\left(1-C_3A'\right)\right]$
C_M*	$\frac{2\alpha}{M}$	$\frac{2\alpha}{MR}\left(R-\frac{2}{3}\right)$	$\frac{2\alpha}{M}\left(1-C_3A'\right)$	$\frac{2\alpha}{MR}\left[R-\frac{2}{3}-C_3A'(R-1)\right]$
c.p.	$\frac{c}{2}$	$\left(\frac{R-\frac{2}{3}}{2R-1}\right)c$	$\left(1-C_3A'\right)\frac{c}{2}$	$\left[\frac{R-\frac{2}{3}-C_3A'(R-1)}{2R-1+C_3A'}\right]c$

$$C_3=\frac{2C_2}{C_1}=\frac{\gamma M^4+(M^2-2)^2}{2(M^2-1)^{3/2}}\ \text{(SEE FIG. 3)}$$

$$A'=\frac{\text{AIRFOIL CROSS-SECTIONAL AREA}}{\text{CHORD SQUARED}}=\frac{A_{CS}}{c^2}$$

VALUES OF A', K_1, AND K_4 (USED LATER)

TYPE OF AIRFOIL	A'	K_1	K_4
DOUBLE WEDGE	$\frac{1}{2}\,t/c$	4	3
MODIFIED DOUBLE WEDGE	$\frac{2}{3}\,t/c$	6	1.5
BICONVEX	$\frac{2}{3}\,t/c$	5.33	1.64

* ABOUT LEADING EDGE

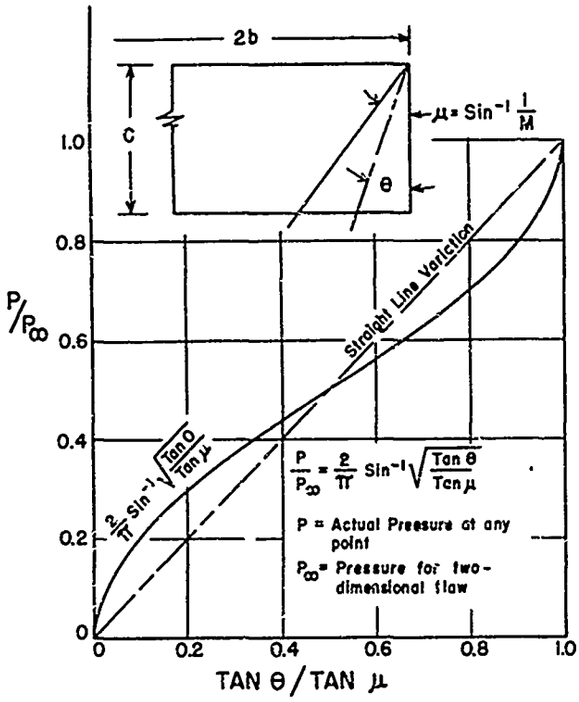

FIG. 1

PRESSURE LOSS DUE TO FLOW AROUND THE TIP

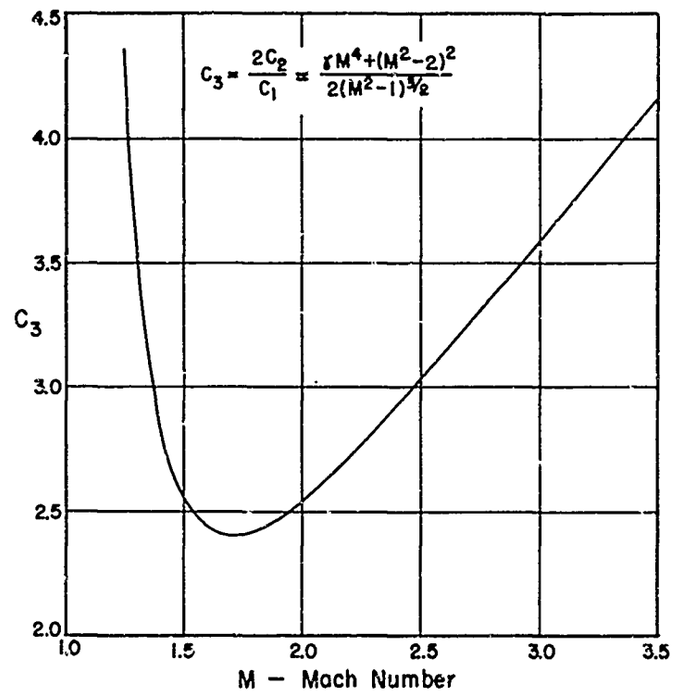

FIG. 2

C_3 versus M

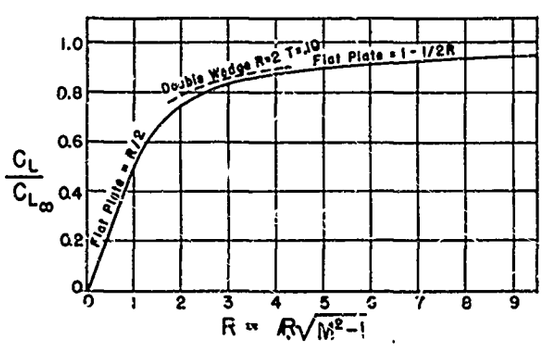

*Wave drag is herein defined as that drag which is caused by the lift of the wing.

FIG. 3

ASPECT RATIO CORRECTION TO LIFT AND WAVE DRAG*

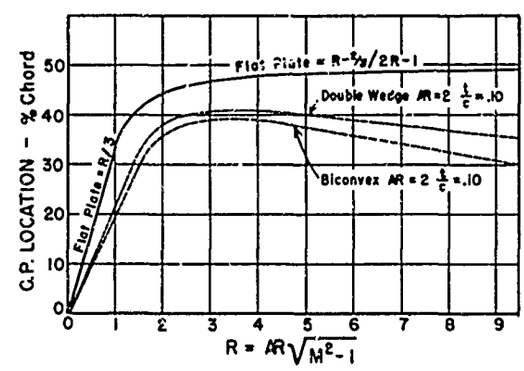

FIG. 4

CENTER OF PRESSURE FOR FINITE ASPECT RATIO

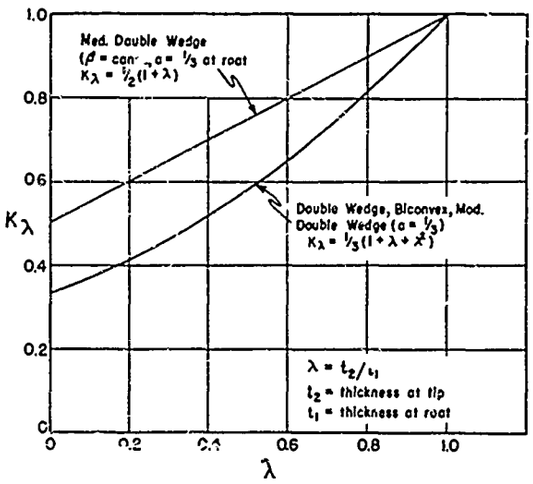

FIG. 5

K_λ's FOR VARIOUS WING SECTIONS (single taper)

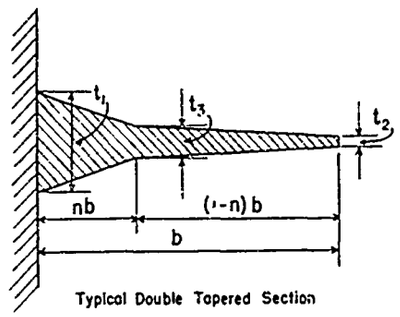

$K_\lambda = nK_{\lambda_B} + (1-n)\lambda_B^2 K_{\lambda_T}$,
where K_{λ_B} and K_{λ_T} can be read from Fig. 5
and $\lambda_B = t_3/t_1$
$\lambda_T = t_2/t_3$

FIG. 6

K_λ's FOR VARIOUS WING SECTIONS (double taper)

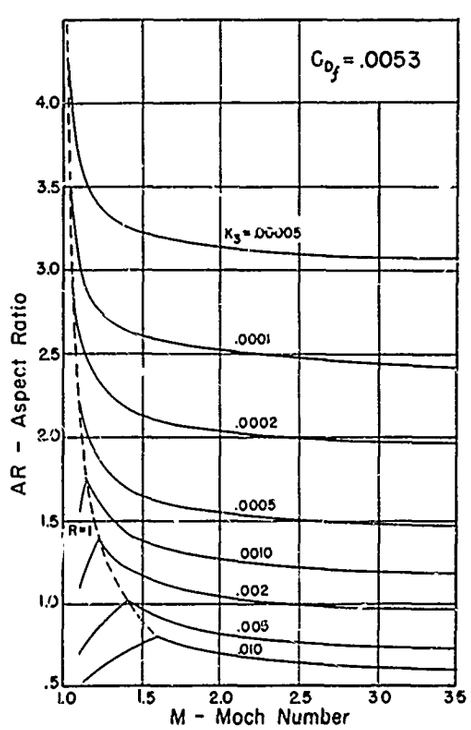

Fig. 7

ASPECT RATIO FOR THIN RECTANGULAR WINGS SUPPORTED OVER ENTIRE BASE

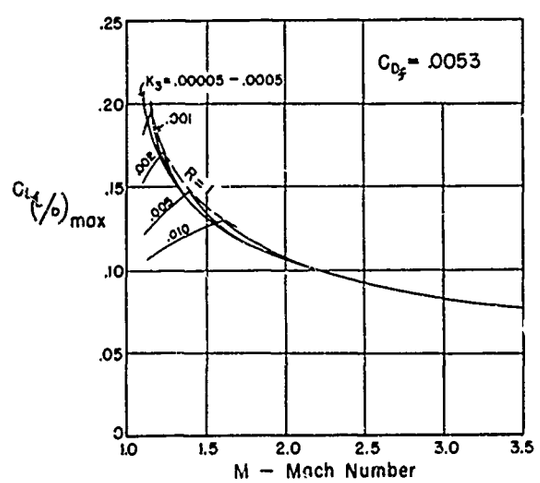

Fig. 8

OPTIMUM LIFT COEFFICIENT —ENTIRE BASE

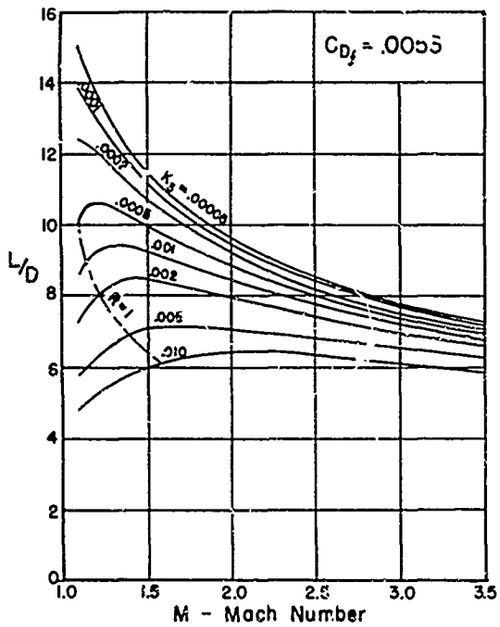

Fig. 9

MAXIMUM LIFT-DRAG RATIO
—ENTIRE BASE

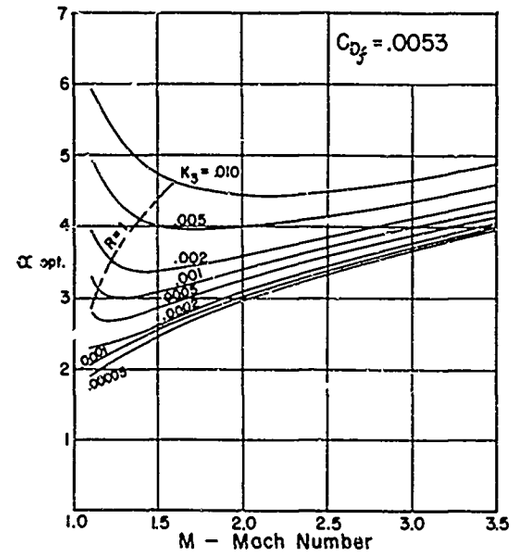

Fig. 10

OPTIMUM ANGLE OF ATTACK
—ENTIRE BASE

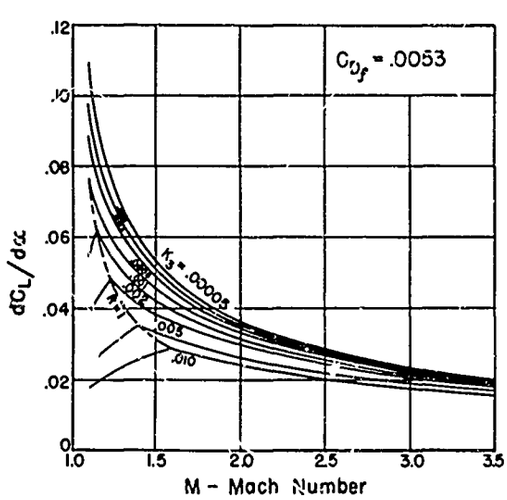

Fig. 11

LIFT CURVE SLOPE
—ENTIRE BASE

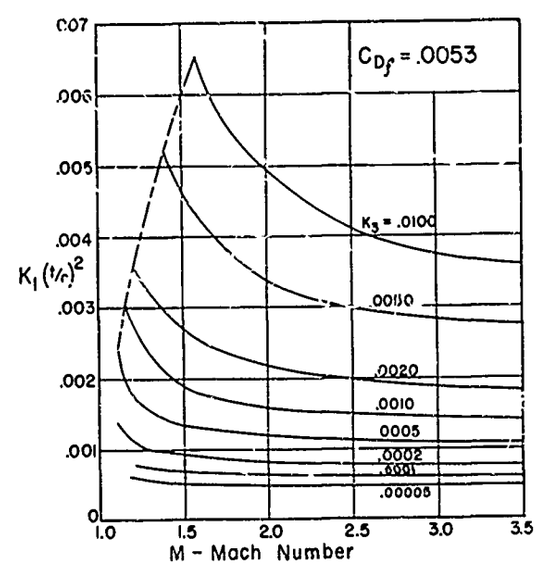

Fig. 12

THICKNESS RATIO
-ENTIRE BASE

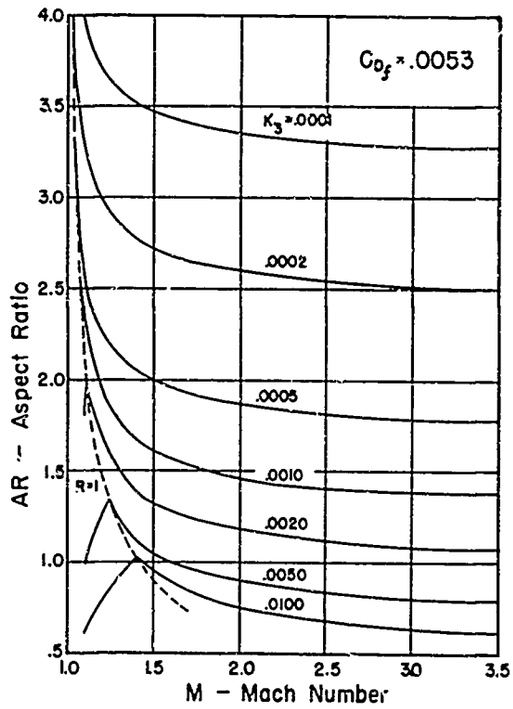

Fig. 13

OPTIMUM ASPECT RATIOS FOR THIN RECTANGULAR WINGS SUPPORTED BY A HUB

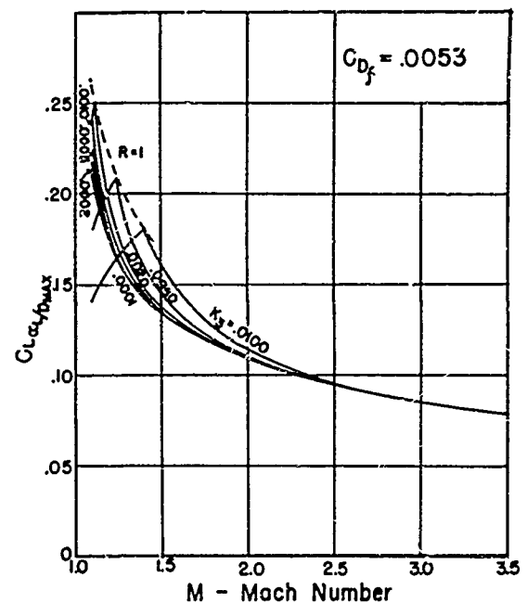

Fig. 14

OPTIMUM LIFT COEFFICIENT — HUB

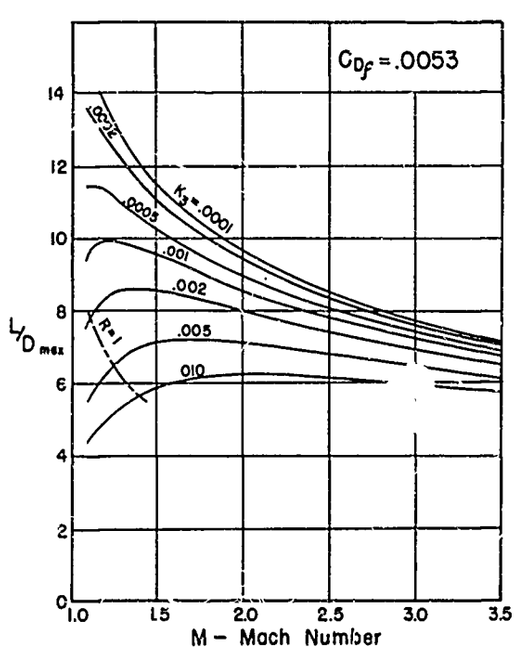

Fig. 15

MAXIMUM LIFT-DRAG RATIO — HUB

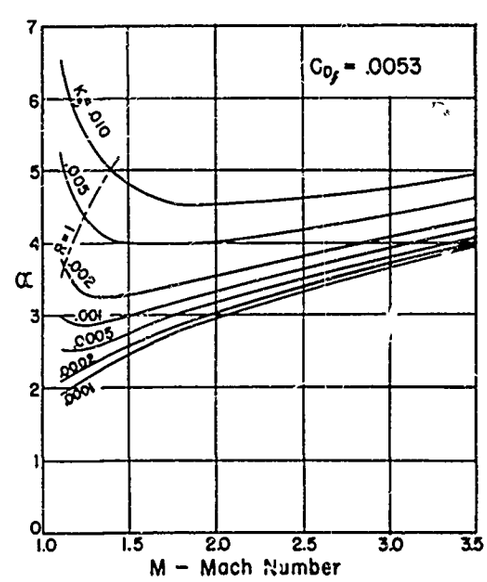

Fig. 16

OPTIMUM ANGLE OF ATTACK — HUB

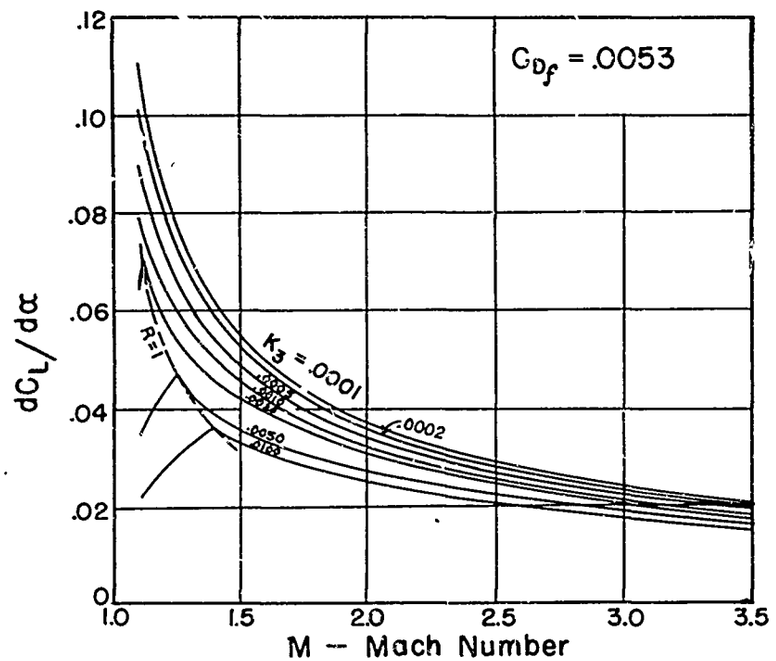

Fig. 17

LIFT CURVE SLOPE
— HUB

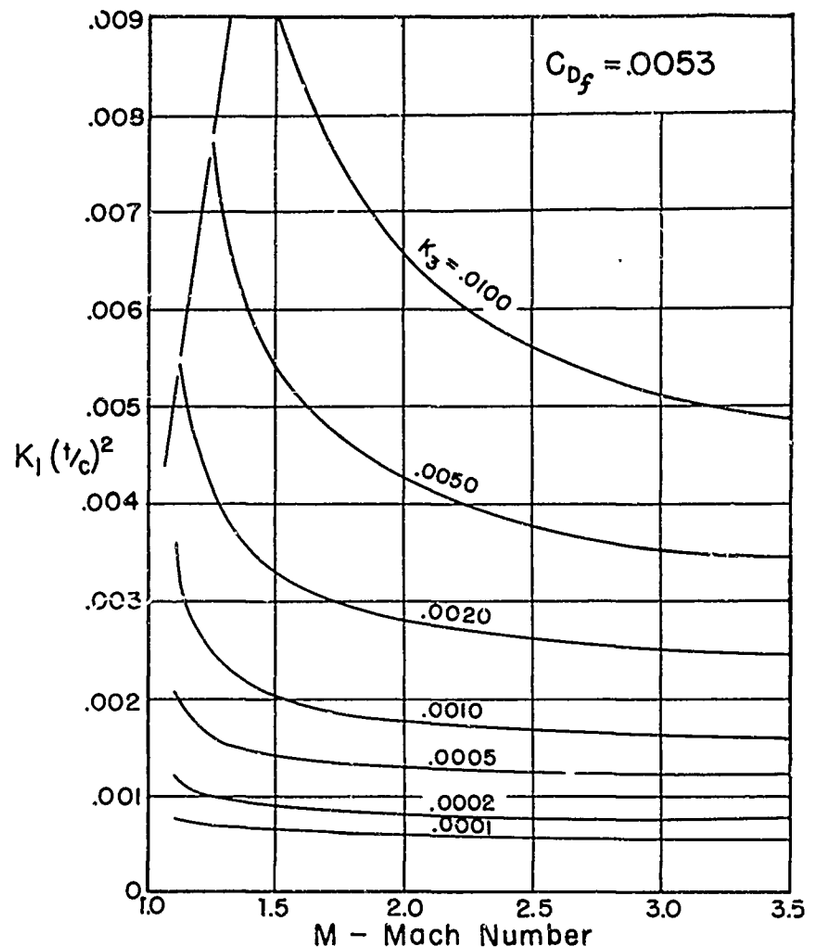

Fig. 18

THICKNESS RATIO
— HUB

III. THE REVERSE DELTA PLANFORM

A section on the "reverse delta" type of wing as discussed in CM-258* was to have been included in this report, however the assumptions made in that paper were not exactly correct, and therefore only a short discussion of this planform will be included here.

The reverse delta wing has the planform of an isoceles triangle with the base facing into the airstream. The angle of the rear surface is greater than the Mach angle so that no tip loss effects will be felt over the surface of the wing. It was assumed in the reference report that this therefore constituted a wing whereon only two-dimensional flow existed and the characteristics corresponded to the two-dimensional case. Actually however, the pressure on a surface behind a yawed corner, such as the aft portion of this type of wing when constructed with a double-wedge section (region B of figure) is a function of the component of Mach number which is normal to the corner, M_N. Furthermore, the pressure inside the Mach cone created at the point of maximum thickness (region C of figure) is of the conical flow type and must be computed by the conical field method. Only in region A is the flow of pure two-dimensional character.

Because of the various types of flow it will be difficult to develop a general expression for form drag and moment coefficient. The design should not be overlooked however, inasmuch as it has distinct structural advantages and the drag may be very little worse than the two-dimensional case. The lift coefficient will be very close to the two-dimensional value, being equal to it for zero thickness. (See figure below)

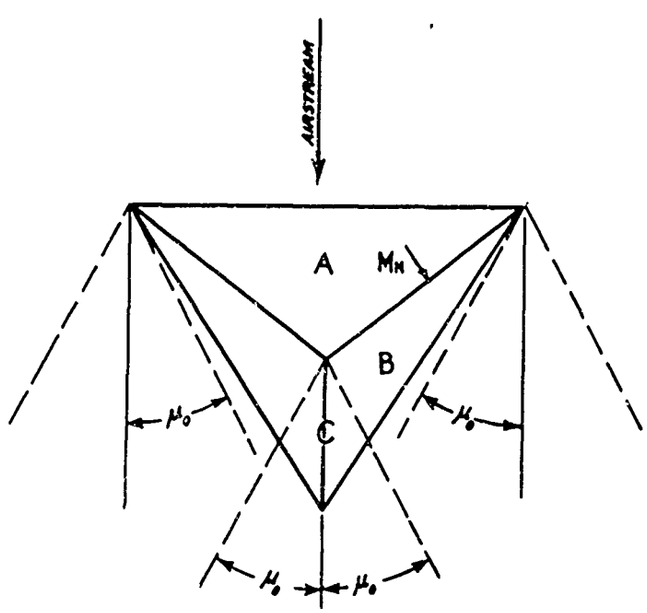

* "Aerodynamic Characteristics of Reverse Arrow Wings at Supersonic Speeds", APL/JHU (May 1946).

IV. LIFT AND DRAG CHARACTERISTICS OF DELTA WINGS AT SUPERSONIC SPEEDS

by E. A. Bonney

Abstract

The lift characteristics of the delta type of wing with the leading edge both inside and outside of the Mach cone from the vertex of the wing have been determined by Stewart (1), Snow (2), and others, and the drag characteristics (for double wedge section only) have been determined by Puckett (3). Using the methods of references (4) and (5), this information is herein used to determine optimum conditions of lift-drag ratio, angle of attack, etc., for comparison with other wing planform shapes. The actual pressure distribution for wings of finite thickness is not known at this writing, and therefore moment and center of pressure data are not included in this report. It is shown that, except for relatively large thickness ratios at low Mach numbers, the delta type of wing has lower values of maximum lift-drag ratio than the reverse-arrow type for which the flow is entirely two-dimensional. The relatively large root chord length required for a given lift is another disadvantage of the delta wing.

The principal advantage of this type of airfoil is in its use as a tail surface due to the aft center of pressure location.

In two reports (6) (7) concerning the lift of delta wings, it has been mentioned that the resultant force on the surface of delta wings entirely inside the Mach cone will be tilted forward of the normal to the chord of the airfoil by an amount which depends on the ratio of the complement of the sweepback angle to the Mach angle, approaching a limit of $\alpha/2$ ahead of the normal for a sweepback angle of 90 degrees. This is due to the subsonic effect wherein the normal Mach number controlling the pressure is less than 1, and will only be possible where the leading edge of the wing is rounded to permit suction peaks similar to the subsonic case.

This effect has not been realized in any tests to date however, and the following analysis assumes that the resultant vector was always at right angles to the chord of the wing.

Assumptions

The assumptions noted in reference (4) concerning separation, skin friction drag coefficient and linearizing trigonometric functions will also be applicable in this report and in addition:

1. The lift curve slope correction for delta airfoils is assumed to be independent of thickness ratio. No sizeable error will result from this assumption because of the small thickness ratios which are used.

2. The slope of the lift curve as derived by Stewart is at an angle of attack of zero degrees. It is assumed here that the slope is constant with angle of attack. This assumption should introduce no sizeable error at the angles for maximum lift-drag ratio which are considered herein.

Nomenclature

The nomenclature of references (4) and (5) is used throughout with the following additions (See also Fig. 13):

ϕ = angle between the leading edge and a normal to the flow direction

$n = \frac{\tan \phi}{M}$ = parameter of leading edge sweepback angle compared with Mach angle

ω_o = planform semi-vertex angle = $90 - \phi$

c = basic chordwise dimension measured from the apex to the position of the tip

l = root chord

r = chordwise distance from most rearward point to point of maximum thickness divided by c

$a = \frac{(c - l)}{c}$

$b = \frac{(l-r)c}{l}$

τ = thickness ratio = t/c

y = distance from wing center line to center of pressure of the semi-span.

Discussion

The delta airfoil consists of a planform shape which is symmetrical about its centerline, pointed at the front, has a sweptback leading edge and straight trailing edge normal to the center line.

For the case where the leading edge is outside of the Mach cone, the lift remains identical in value, but not in distribution (2) to the two-dimensional case. The form drag, however, is slightly higher, hence the maximum lift-drag ratio will be slightly lower than for the reverse arrow type for which two-dimensional lift and drag apply.

For delta shapes where the leading edge is inside the Mach cone, the lift curve slope will decrease from the two-dimensional value by an amount which is a function of the ratio of the leading edge sweepback angle to the complement of the Mach angle (defined by the parameter "n") as shown in Fig. 1 (1). (Note that when n = 1, the sweepback angle is just equal to the complement of the Mach angle, and n = 0 corresponds to a straight leading edge.) The form drag will also be a function of "n" as well as being a function of the thickness ratio, location of point of maximum thickness, and Mach number. The coefficient of form drag was determined in reference (3) and is shown in Fig. 2. It can be seen that for large values of n, the form drag is greatly reduced from the optimum two-dimensional value, where n = 0. Hence, for conditions of high wing loadings where the required thickness ratio becomes large and form drag becomes a big proportion of the total drag for optimum lift-drag conditions, the delta type of wing design will theoretically show up to advantage over the reverse arrow type in the lower range of Mach numbers. However, for most practical thickness ratios and Mach numbers, the reverse arrow will still give higher lift-drag ratios as shown in Figs. 3, 4, and 7. A definite disadvantage of the delta wing where n is large is the relatively large root chord length required for a given lift. The center of pressure travel of this type will probably be large also due to the large chord length and the odd type of pressure distribution (2) with the leading edge either inside or outside the Mach cone.

It is to be noted that this analysis is for the double wedge type of airfoil cross-sectional shape only, but the results obtained herein will be qualitatively comparable for any type of cross-section.

Figure 3 shows the actual thickness ratios at which the delta type of airfoil with n = 1.3 and 2.5 will be superior to the reverse arrow type while Fig. 4 shows the same effect when considered from the aerodynamic-strength combination standpoint. Limiting values of K_3 at n = 0, 1.3, 1.7, and 2.5 are shown for purposes of comparison. Fig. 5 shows the maximum lift-drag ratios for the range of practical values of K_3 for values of n = 1.3 and 2.5.

A comparison of the maximum lift-drag ratios of delta and reverse arrow wings is shown in Fig. 7. The improved characteristics of the delta type wing for high thickness ratios at low Mach numbers is evident from the curves.

In references (4) and (5), the following expressions were derived for lift and drag coefficients:

$$C_L = \frac{4\alpha}{M}\left(\frac{C_L}{C_{L\infty}}\right), \quad (\alpha \text{ in radians})$$

$$C_D = \frac{K_1 \tau^2}{M} + \frac{4\alpha^2}{M}\left(\frac{C_L}{C_{L\infty}}\right) + C_{D_f} \text{ and}$$

$$C_D = \frac{K_3 AR^2}{M} + \frac{4\alpha^2}{M}\left(\frac{C_L}{C_{L\infty}}\right) + C_{D_f}$$

Equation (3) applies for wings supported over their entire base. K_3 will be evaluated below.

The optimum angle of attack is,

$$\alpha_{opt} = 28.65\sqrt{\frac{K_3 AR^2 + C_{D_f} M}{C_L/C_{L\infty}}}$$

and the maximum lift-drag ratio becomes

$$\frac{L}{D}_{max} = \sqrt{\frac{C_L/C_{L\infty}}{K_3 AR^2 + C_{D_f} M}}$$

Values of $C_L/C_{L\infty}$ and K_1 can be read directly from Figs. 1 and 2 respectively. The skin friction drag coefficient is taken as .0053, as in references 4 and 5. The aerodynamic-strength parameter K_3 is dependent on the spanwise pressure distribution as shown in the following derivation:

$$s = \frac{ct^2}{24} = \frac{m}{S} = \frac{wbc}{2} \times b \times \frac{y}{b} \times \frac{1}{S}$$

where y/b is the ratio of the distance between the wing center line and the center of pressure, to the wing semi-span.

By the methods of reference (2)*, it may be shown that, for wings whose leading edges are outside of the Mach cone,

$$y = \frac{2c}{3}\,\bar{\tau}$$

* This reference considers the distribution over a flat plate only. However it is assumed here that the spanwise variation will be similar for a wing having a finite thickness.

where $\bar{t}$ is found as the limiting case of equation (28) of that reference to be

$$\bar{t} = \frac{1}{\pi} \tan \mu \left(1 + \frac{2\beta}{\sin 2\beta}\right)$$

In the above terminology, is defined as follows:

$$\cos\beta = \frac{1}{\pi \tan \omega_0}$$

Therefore

$$\frac{y}{b} = \frac{2}{3\pi} \cos\beta \left(1 + \frac{2\beta}{\sin 2\beta}\right)$$

The variation of y/b with β as defined above will be found plotted in Fig. 13.

Now from equation (6),

$$\frac{t^2}{c^2} = \tau^2 = \frac{3\, w AR^2}{4\, S} \frac{y}{b}$$

$$\text{Then } K_3 = \frac{K_1 K_4 w}{8 S} \frac{y}{b}$$

where $K_4 = 6$ as in references 4 and 5.

For the case of the delta airfoil entirely inside the Mach cone, reference 5 indicates that the value of y/b for large values of n is the same as calculated above at n = 1.0 (= 0), namely,

$$\frac{y}{b} = \frac{4}{3\pi} = .4244$$

Inasmuch as the slope of the curve of Fig. 13 is 0 at $\beta = 0$, it will be assumed that this value is constant for any value of n greater than 1.0, i.e., all cases of leading edge inside the Mach cone. Therefore the expression for K_3 will be:

$$K_3 = \frac{K_1 K_4 w}{18.85 S}$$

Since the original preparation of this report, additional calculations for the characteristics of the delta wing with the trailing edge swept forward and backward have been carried out by Dr's. Puckett and Stewart (8) and they have very kindly consented to the inclusion of this information in this report. These data will be found in Figures 13 through 22. No general study of optimization has been made due to the detailed investigation involved.

References

1. Stewart, H. J. "The Lift of Delta Wings at Supersonic Speeds", Journal of Applied Mathematics, Oct. 1946, p. 246.

2. Snow, R. M., "Application of Busemann's Conical Field Method to Thin Wings of Polygonal Planform", CM-265 Applied Physics Laboratory, May 23, 1946. (This paper is reprinted as Section I of this report)

3. Puckett, A. E., "Supersonic Wave Drag of Thin Airfoils", (December 26, 1945). Paper presented at a meeting of the Institute of Aeronautical Sciences, January 1946.

4. Bonney, E. A., "Aerodynamic Characteristics of Solid, Rectangular Airfoils at Supersonic Speeds", CM-247 Applied Physics Laboratory, May 6, 1945. (This paper is reprinted as Section II of this report.)

5. Bonney, E. A., "Aerodynamic Characteristics of Reverse-Arrow Wings at Supersonic Speeds", CM-258 Applied Physics Laboratory, May 14, 1946.

6. Jones, R. T., "Properties of Low-aspect-ratio Pointed Wings at Speeds Below and Above the Speed of Sound", NACA ACR No. L5F13, June, 1945.

7. Hayes, W. B., Browne, S. H., and Lew, R. J. "Linearized Theory of Conical Supersonic Flow With Application to Triangular Wings" NA-46-818. Sept. 30, 1946.

8. Stewart, H. J. and Puckett, A. E., "Aerodynamic Performance of Delta Wings", (This paper presented at Institute of Aeronautical Science 15th annual meeting, New York, January 1947).

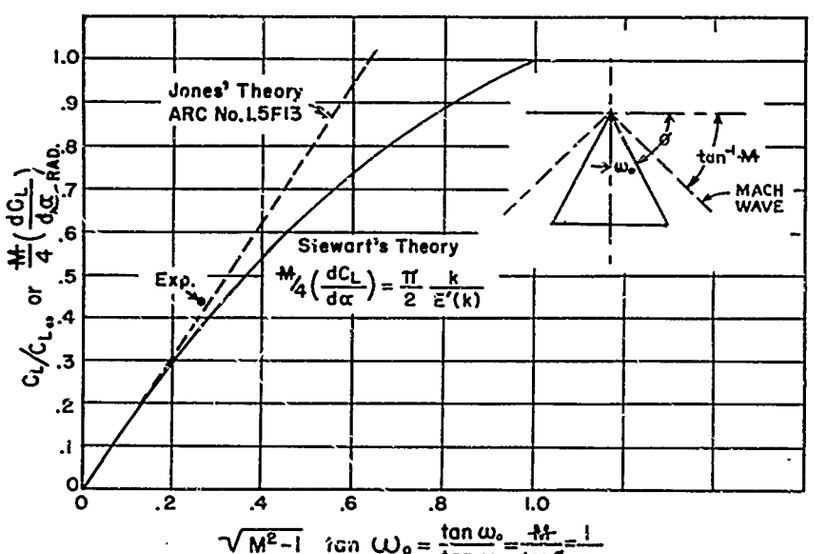

Fig. 1
LIFT CHARACTERISTICS OF Δ WINGS

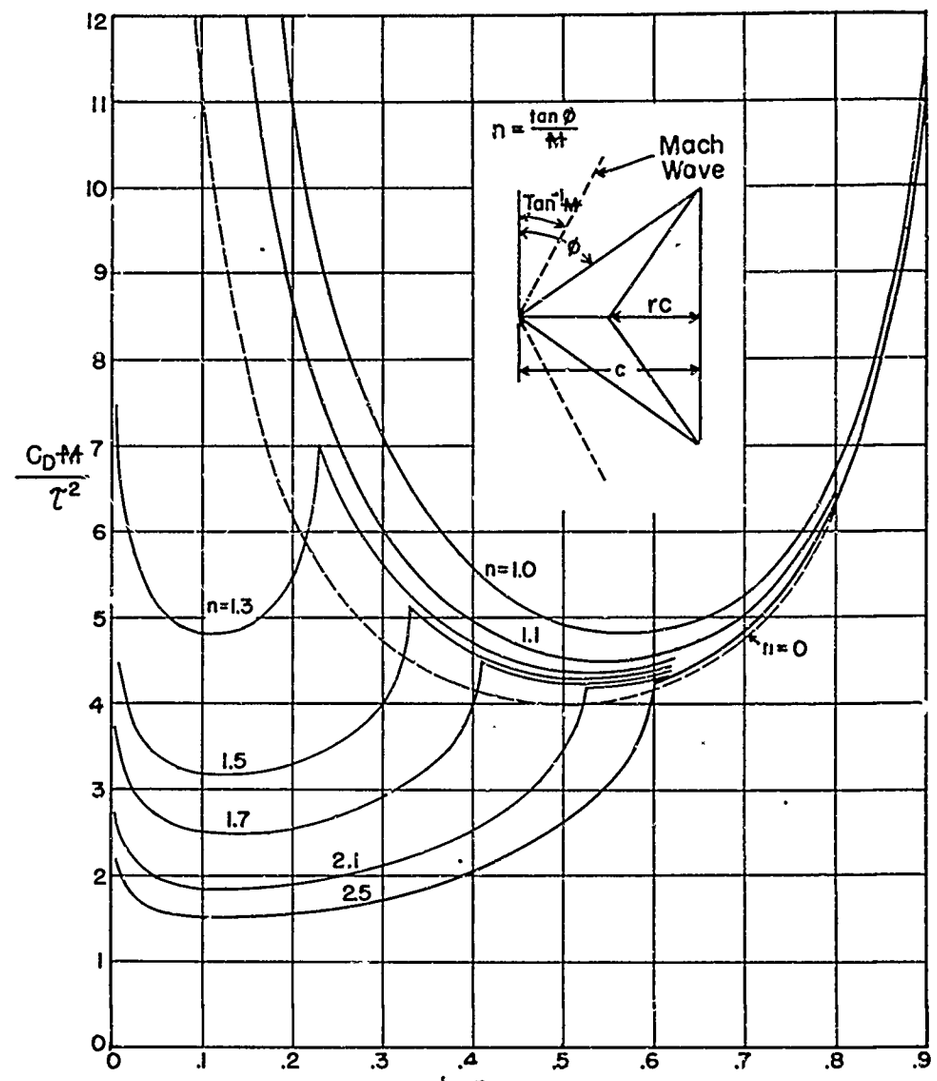

Fig. 2
FORM DRAG OF DELTA AIRFOILS WHOSE LEADING EDGES ARE INSIDE THE MACH CONE

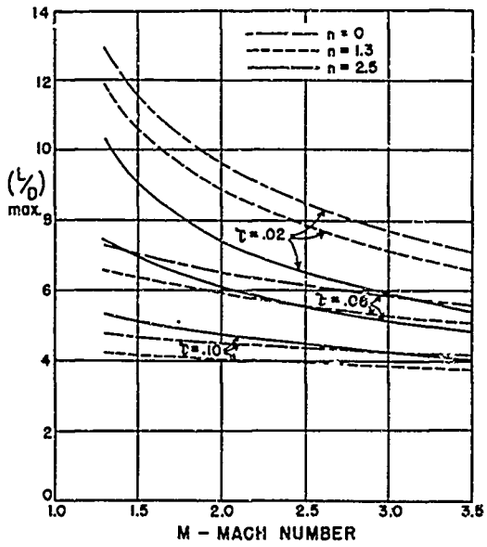

Fig. 3
LIFT-DRAG RATIO OF DELTA AND RECTANGULAR WINGS

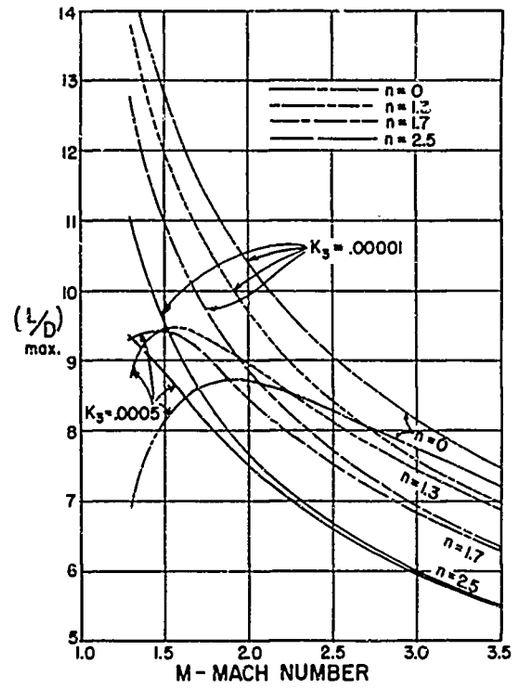

Fig. 4
MAXIMUM LIFT-DRAG RATIO — DELTA WINGS

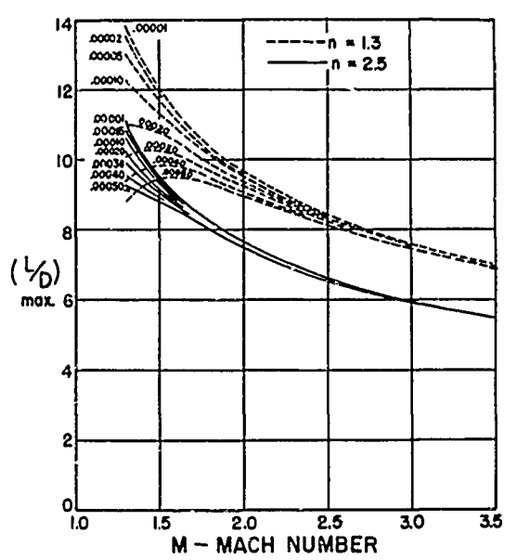

Fig. 5
MAXIMUM LIFT-DRAG RATIO

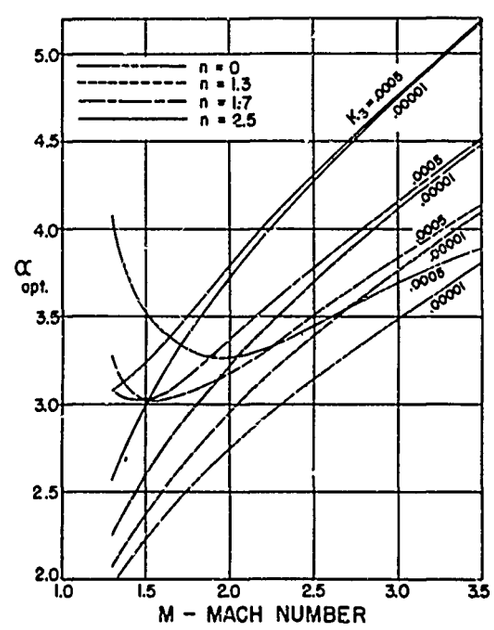

Fig. 6
OPTIMUM ANGLE OF ATTACK — DELTA WINGS

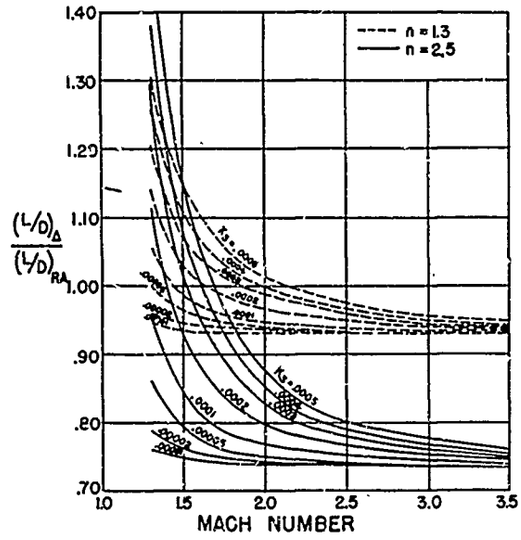

Fig. 7
RATIO OF MAXIMUM LIFT-DRAG RATIOS OF DELTA AND REVERSE ARROW WINGS

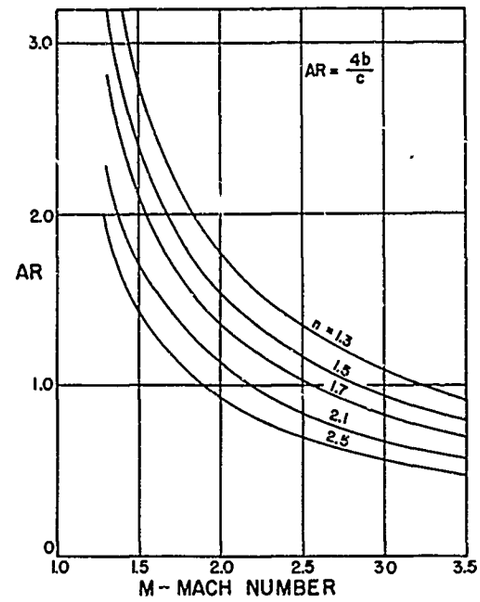

Fig. 8
ASPECT RATIO OF DELTA WINGS

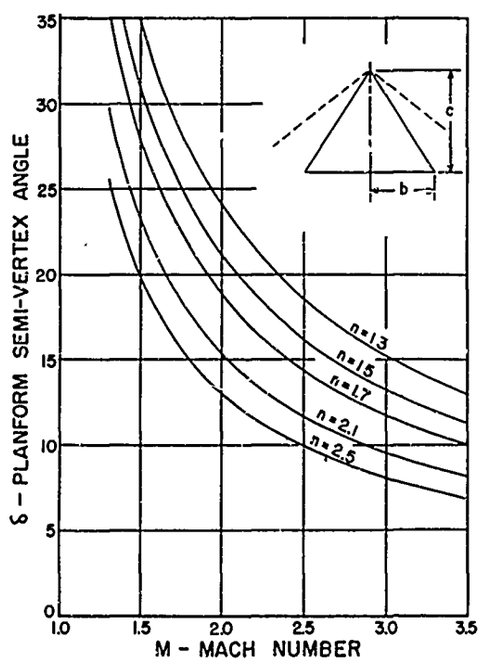

Fig. 9
PLANFORM SEMI-VERTEX ANGLE OF DELTA WINGS

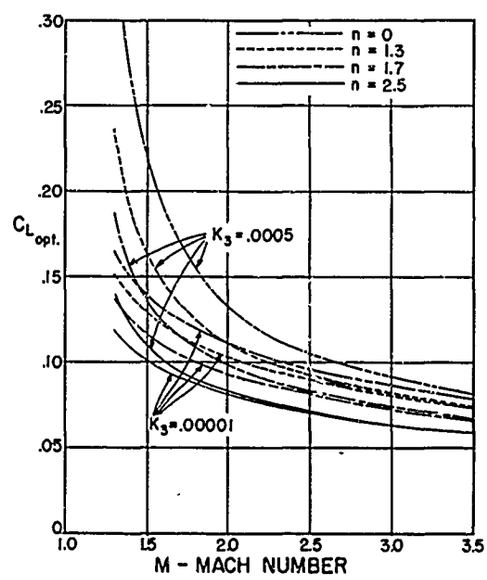

Fig. 10
OPTIMUM LIFT COEFFICIENT —DELTA WINGS

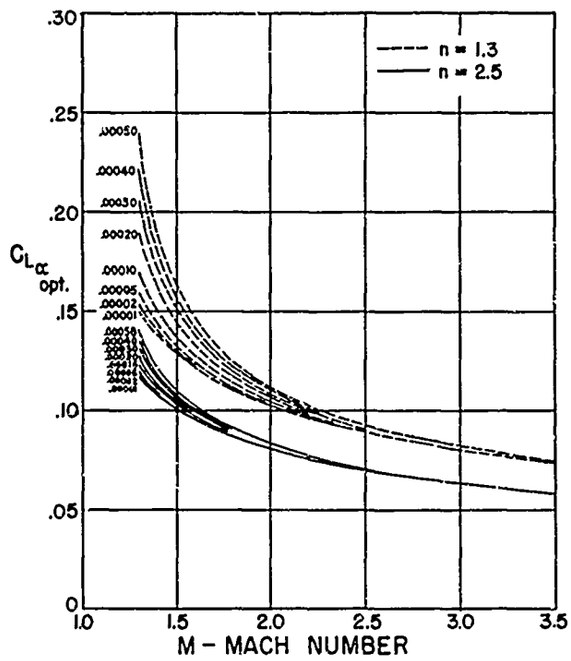

Fig. 11
OPTIMUM LIFT COEFFICIENT

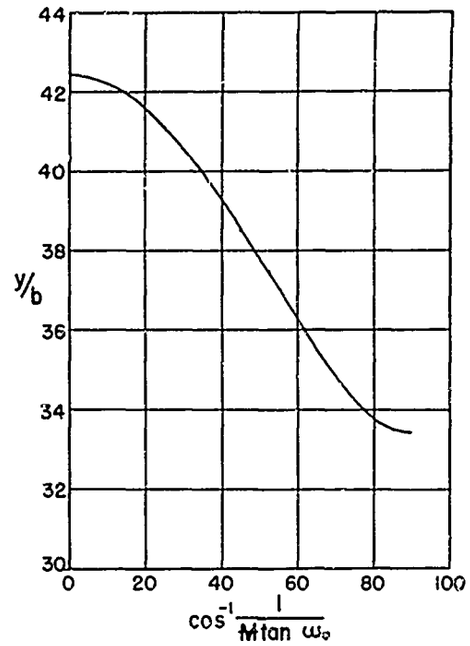

Fig. 12
SPANWISE CENTER OF PRESSURE
LOCATION - DELTA WINGS

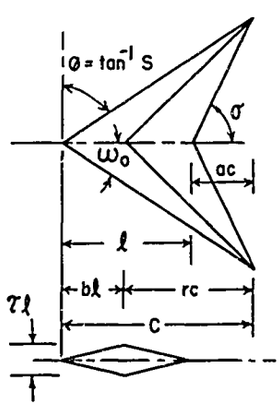

Fig. 13

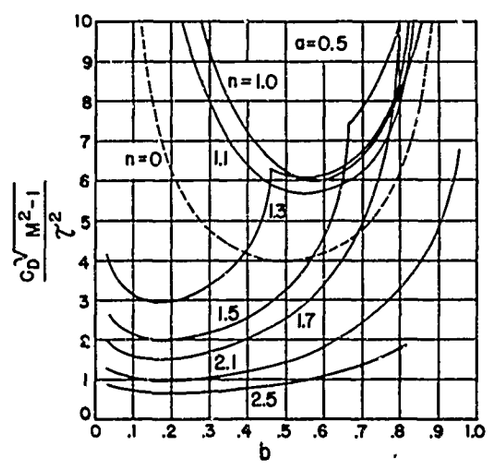

Fig. 14
Δ-WING DRAG VERSUS
MAXIMUM THICKNESS POSITION

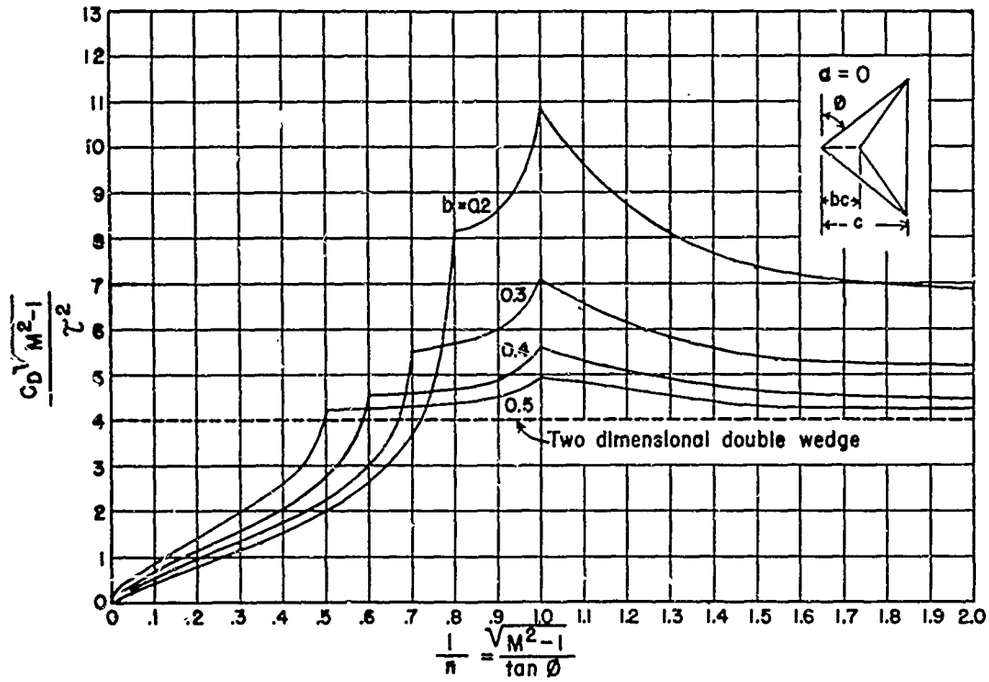

Fig. 15
Δ-WING DRAG

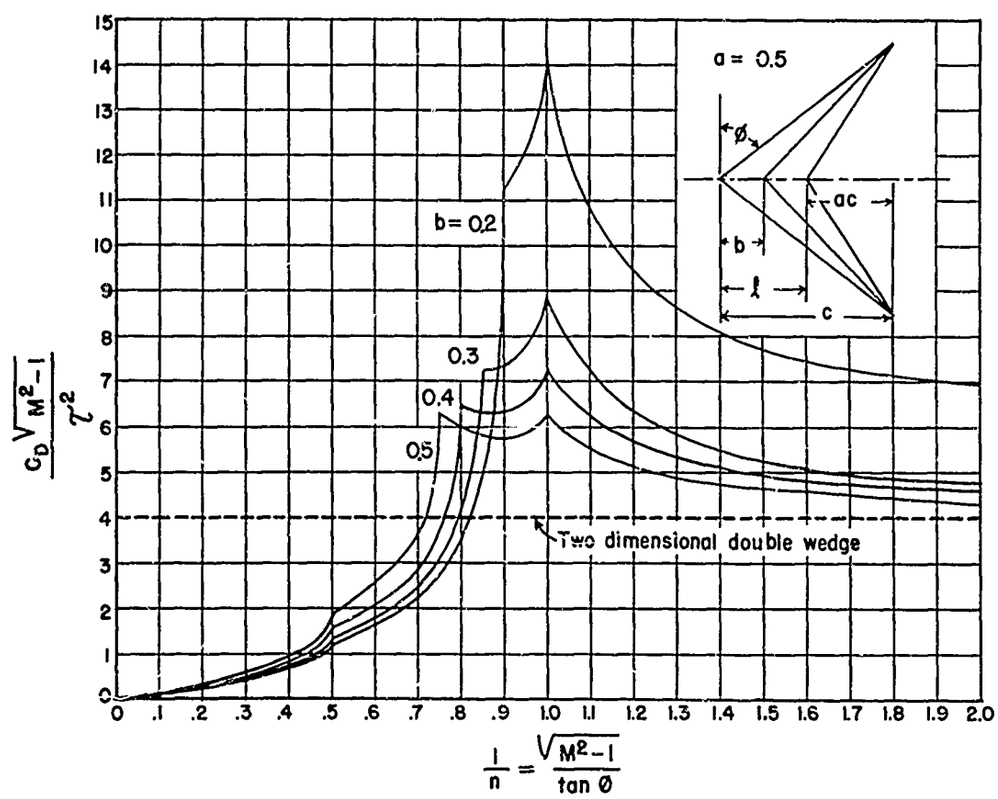

Fig. 16
Δ-WING DRAG-SWEPT TRAILING EDGE

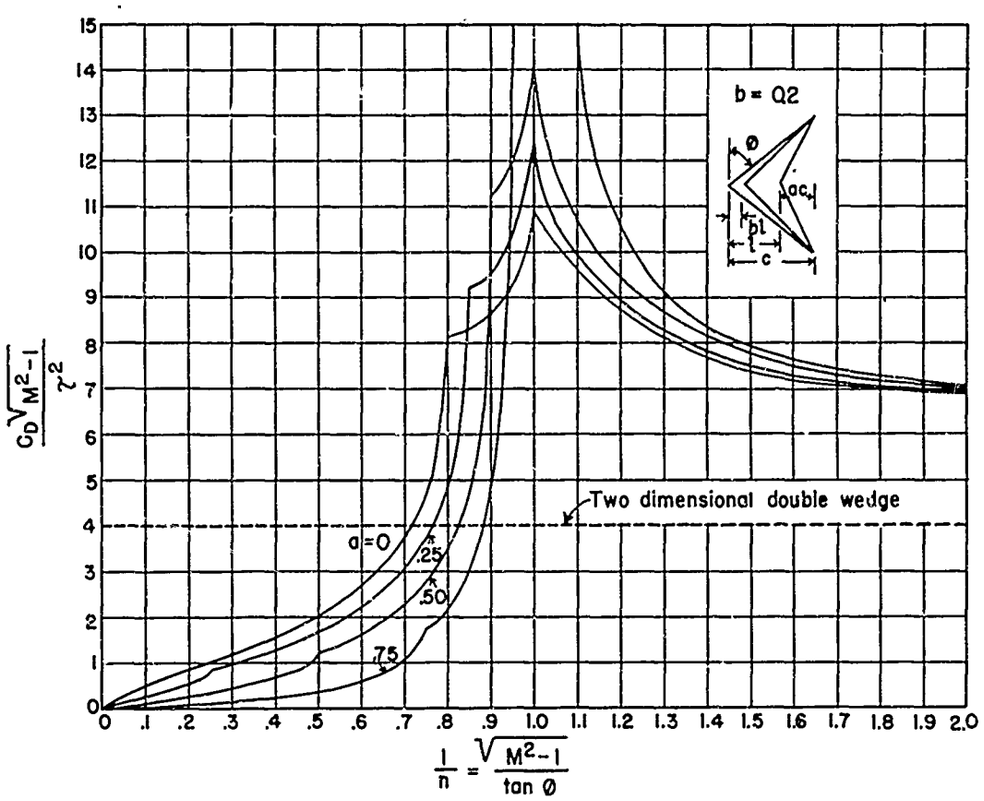

Fig. 17
Δ-WING DRAG-SWEPT TRAILING EDGE

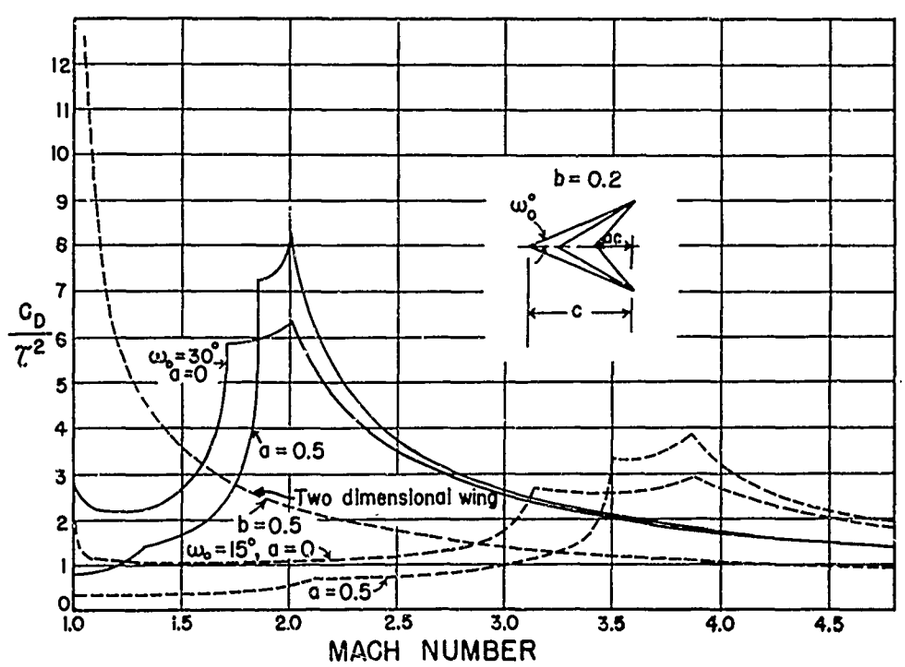

Fig. 18
Δ-WING DRAG

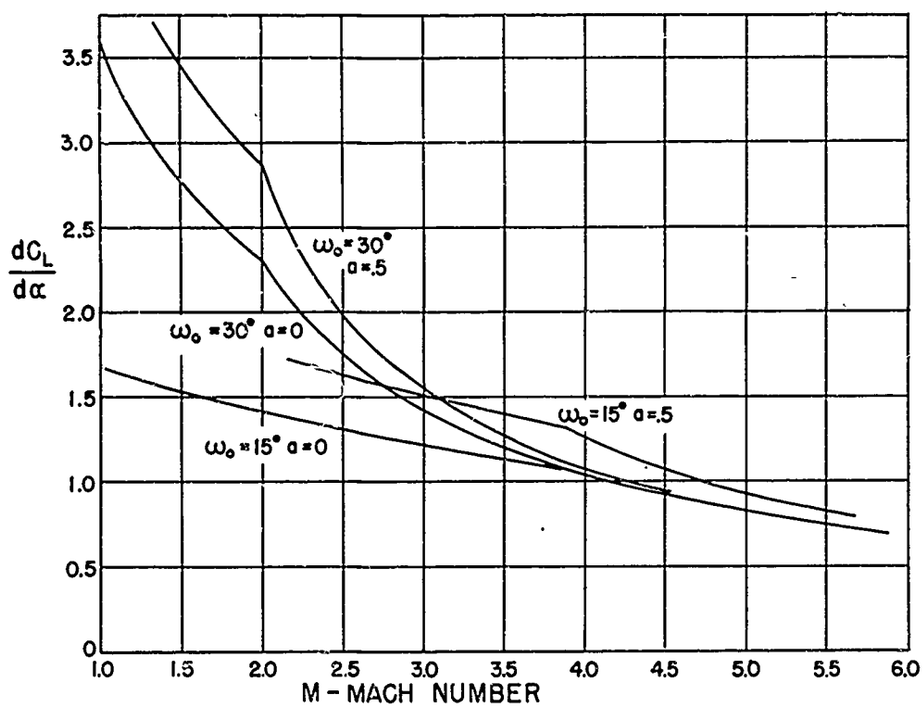

Fig. 19

LIFT CURVE SLOPE
DELTA AND ARROWHEAD PLANFORMS
(Fixed Planforms)

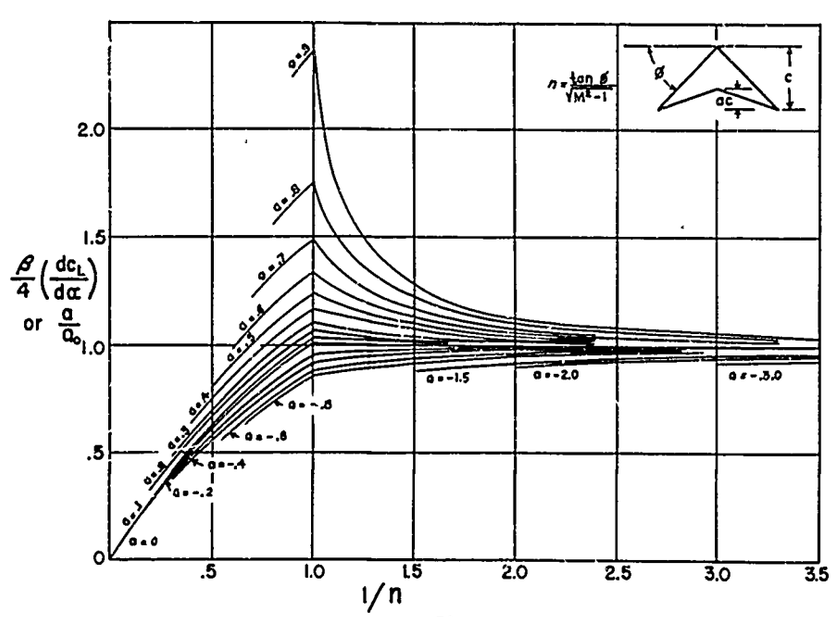

Fig. 20

LIFT CURVE SLOPE
DELTA AND ARROWHEAD PLANFORMS

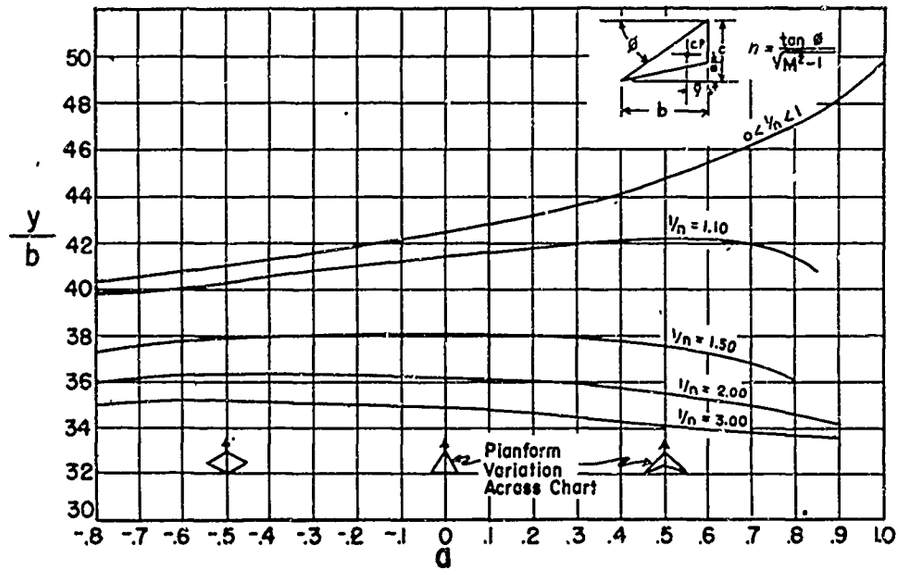

Fig. 21

SPANWISE CENTER OF PRESSURE LOCATION
DELTA AND ARROWHEAD PLANFORMS

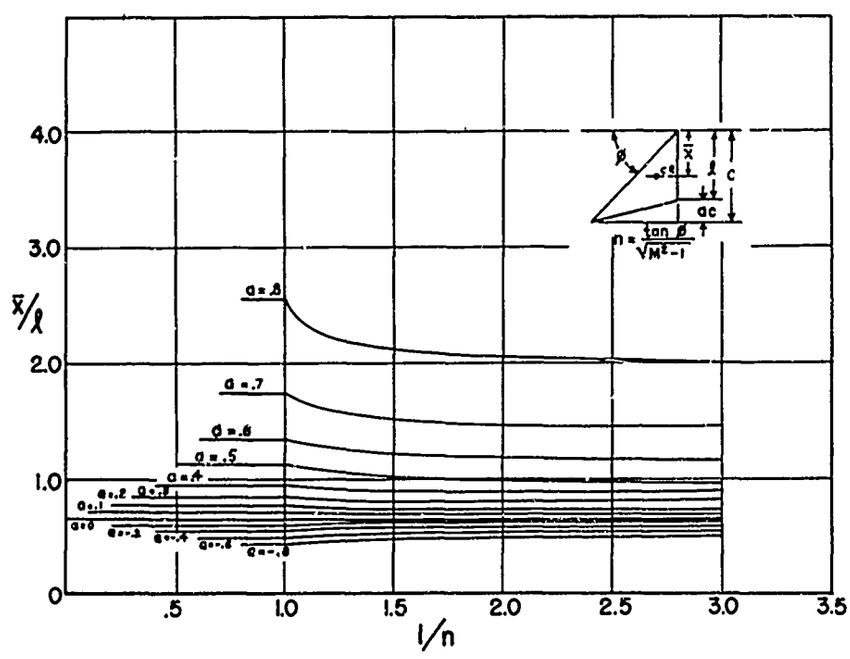

Fig. 22

CHORDWISE CENTER OF PRESSURE LOCATION
DELTA AND ARROWHEAD PLANFORMS

V. SECTIONAL CHARACTERISTICS OF STANDARD AIRFOILS

by E. A. Bonney

In selecting the optimum cross-sectional shape of airfoil for use in supersonic flight, one is tempted to choose the double-wedge type because of its low form drag per unit thickness. This is a fallacy because drag per unit stress is the proper criterion for design. The increased drag of other types must be balanced against their increased strength (section modulus) to determine the optimum shape.

With this in mind, the following table and curves have been constructed to show the relation between drag, stress, and thickness ratio for various types of airfoils including one designed by Dr. A. E. Puckett in which the optimum shape to give minimum drag per unit stress was the design criterion. It is shown that the optimum shape is only very slightly (0.7 per cent) better than the biconvex (double circular arc) section. For practical purposes, therefore, (inasmuch as the Puckett wing would be difficult to machine) the biconvex type of cross-section is the optimum shape of airfoil for a given allowable stress at the root of the wing.

Shape	Biconvex	Optimum (Puckett)	Double Wedge	Modified Double Wedge $a = 1/3$ *	Modified Double Wedge 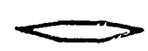
s	$\frac{ct^2}{13.125}$	$\frac{ct^2}{13.87}$	$\frac{ct^2}{24}$	$\frac{ct^2}{12}$	$\frac{ct^2}{12}(2-3a)$
$\frac{s}{c^3}$	$\frac{\tau^2}{13.125}$	$\frac{\tau^2}{13.87}$	$\frac{\tau^2}{24}$	$\frac{\tau^2}{12}$	$\frac{\tau^2}{12}(2-3a)$
⊗ $\frac{c_{D_0}\sqrt{M^2-1}}{4}$	$1.333\tau^2$	$1.253\tau^2$	τ^2	$1.5\tau^2$	$\frac{\tau^2}{2a}$
⊗ $\frac{c_{D_0}\sqrt{M^2-1}}{4}$	$\frac{17.50\,s}{c^3}$	$\frac{17.38\,s}{c^3}$	$\frac{24\,s}{c^3}$	$\frac{18\,s}{c^3}$	$\frac{6\,s}{a(2-3a)c^3}$

* a = fraction of chord length having wedge shape (each end)

⊗ c_{D_0} – for infinite span ratio

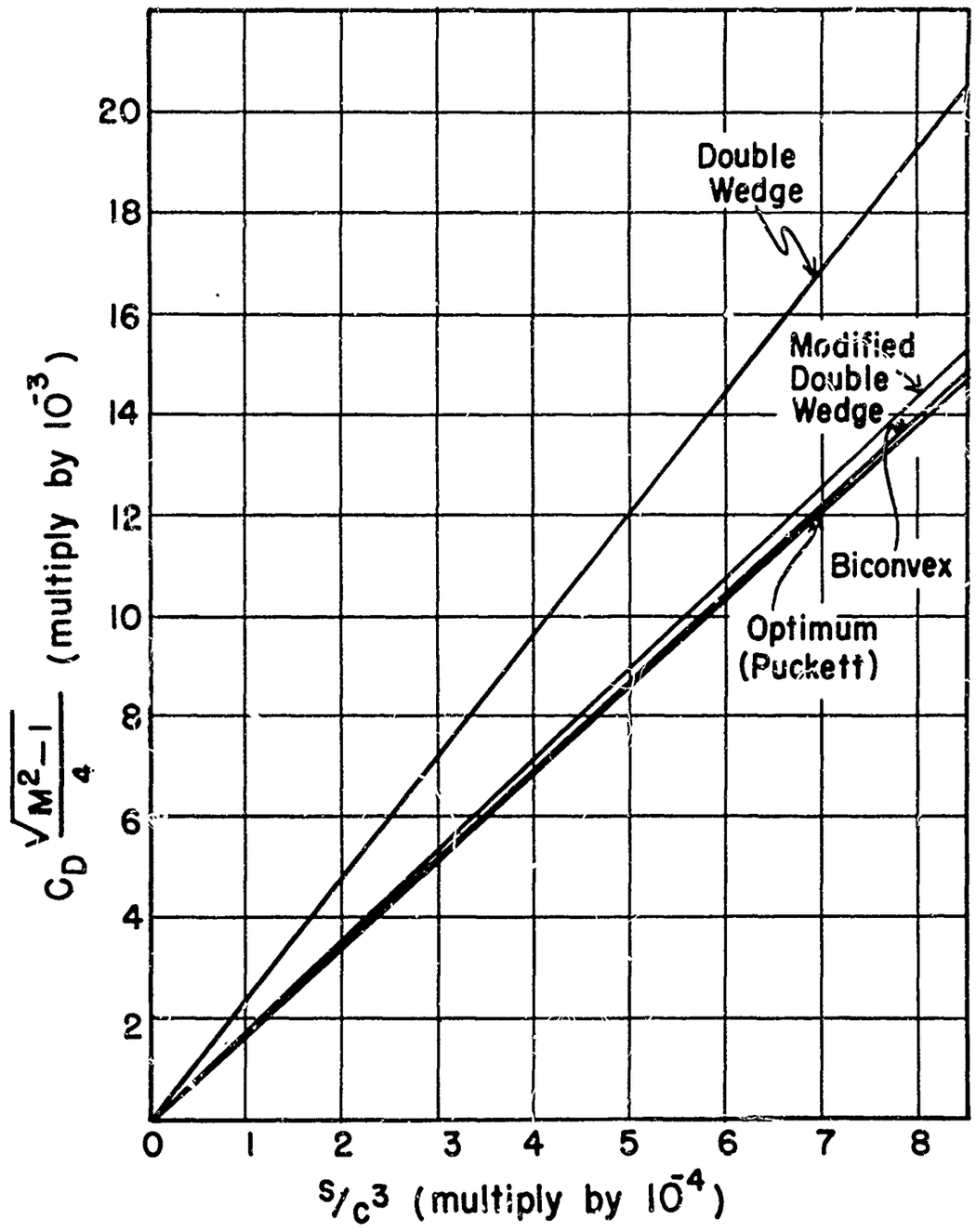

Fig. 1

DRAG COEFFICIENT VS STRESS

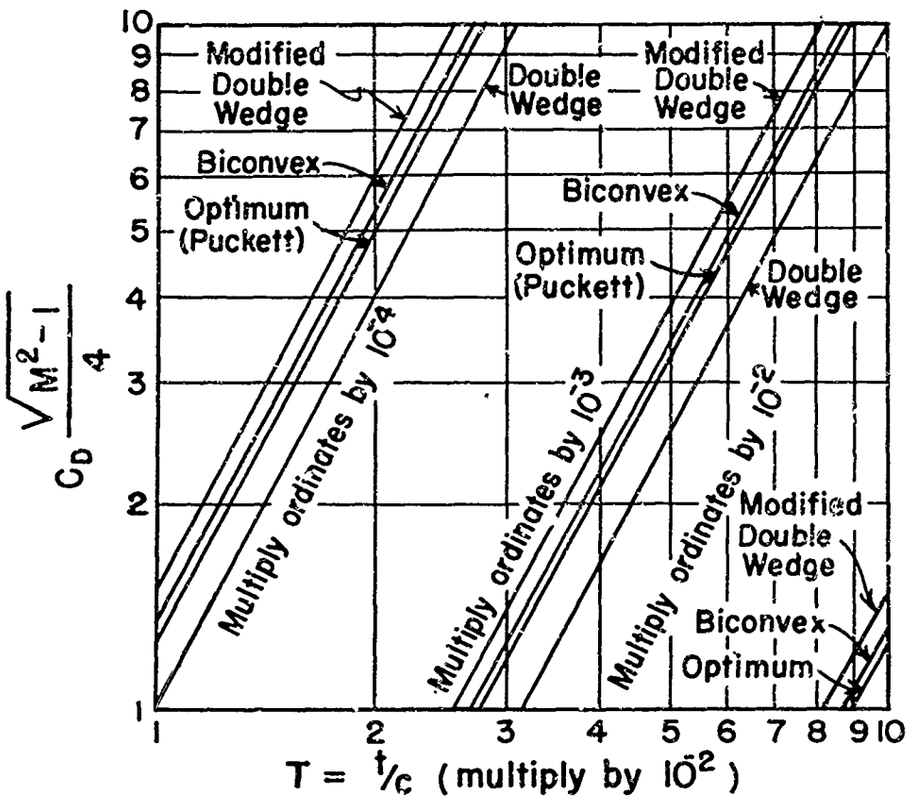

Fig. 2

DRAG COEFFICIENT VS THICKNESS RATIO

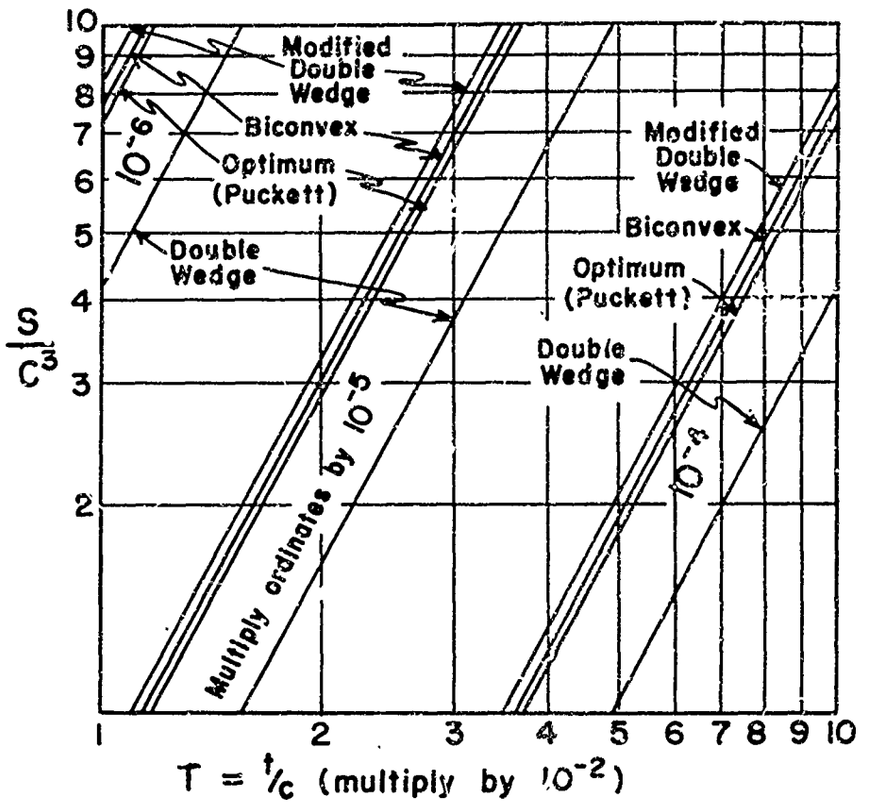

Fig. 3

STRESS VS THICKNESS